2010

Water and solute transport in the shallow subsurface of a riverine wetland natural levee

April Elea Newman
Louisiana State University and Agricultural and Mechanical College

WATER AND SOLUTE TRANSPORT IN THE SHALLOW SUBSURFACE OF A RIVERINE WETLAND NATURAL LEVEE

A Thesis

Submitted to the Graduate Faculty of the
Louisiana State University and
Agricultural and Mechanical College
in partial fulfillment of
requirements for the degree of
Master of Science

in

The School of Renewable Natural Resources

by
April Newman
B.S., University of Nevada, Las Vegas 2002
May 2010

ACKNOWLEDGEMENTS

There are many people to whom I am grateful for supporting and encouraging my professional and scholarly pursuits. My first and most fervent supporter is my mother, Pam, who set me on this path by reading to me relentlessly, taking me to the woods, and helping me recognize my natural talents and interests. Also integral to my success is my husband Jason, who has been by my side now for fourteen years (almost half of my young life) and whose insightful advice steers my most important life decisions.

I recognize the immeasurable value of mentors in my development as a hydrologist and a scientist. Books, courses, and self-motivation will only carry one so far, and it often takes a dedicated teacher and advocate to facilitate further advancement in a career or a discipline. Of these, I give thanks and admiration to Mike Mathews, whose enthusiasm for hydrology I share and to whose leadership abilities I aspire. I am also grateful to my advisor on this project, Dr. Richard Keim, who stokes my insatiable curiosity and has probably taught me more than any other single individual.

I am inspired by all those I have encountered, too numerous to name, who passionately endeavor to make a positive difference in the world; when worldly woes seem overwhelming, I find strength in the tenacity of the do-gooders. To all of you whose daily tasks are devoted to something larger than yourself: Namaste.

TABLE OF CONTENTS

LIST OF TABLES

LIST OF FIGURES

ABSTRACT

In riverine wetlands, the rate and magnitude of water exchanged between river channels and adjacent wetlands have a major influence on hydrologic function and associated aquatic habitat and water quality. River channels are generally separated from backswamps by natural levees; however, preferential flow may allow potentially substantial water and solute exchange between them. Determining the influence of preferential flow on water and solute transport in natural levees requires an innovative approach that allows measurement of transport rates at a scale large enough to capture field-scale variability.

To test the hypothesis that preferential flow is important to subsurface water movement through natural levees, we measured hydraulic gradients and solute tracers in a 10 x 9 m grid of 19 shallow (2m) monitoring wells within a large volume (300 m^3) of natural levee in the Atchafalaya Basin, Louisiana. In addition to measuring transient responses to natural events, we constructed a small reservoir on the backswamp side of the levee to create a hydraulic gradient from the swamp to the adjacent river channel. We used a simple linear system approach to model residence time distributions of water and solute within the natural levee.

Overall, hydraulic response to forcing events, whether from rain or reservoir filling, was rapid in all wells (mean pressure wave velocity 2.5 E-2 m/s) and relatively uniform; in comparison, tracer transport was much slower (mean 3.2 E-4 m/s) and more variable. Spatially, mean subsurface tracer velocities varied over several orders of magnitude: between 1.6 E-7 and 6.8 E-5 m/s under a 12-cm hydraulic gradient and between 2.1 E-7 and 2.2 E-3 m/s under a 70-cm hydraulic gradient.

Comparatively greater variability of chemical verses hydraulic behavior indicates multiple functioning transport mechanisms in natural levee sediments and suggests preferential flow; thus, methods that estimate transport rates based on standard point measurements likely greatly underestimate exchange at the field scale. Results suggest that preferential, subsurface flow through natural levees may provide hydrologic connectivity that is meaningful to basin-scale biogeochemical processes.

INTRODUCTION

In riverine wetlands, the rate and magnitude of water exchanged between river channels and adjacent wetlands have a major influence on hydrologic function and associated aquatic habitat and water quality (Sabo et al., 1999). Backswamps are separated from river channels by natural levees that form during bank overflow events. When water levels are high, surface connectivity allows overflow flooding, but once river levels drop, surface connections are reduced or eliminated. Based on the well-documented hydrologic effects of canals and spoil banks (Deegan et al., 1984; Hopkinson and Day, 1980), the conventional conceptual framework of riverine swamp hydrology is that natural levees greatly impede or eliminate connectivity between wetlands and river channels.

Connectivity between backswamps and stream channels has important implications for biogeochemical processes, and thus for water quality. Natural levees, the interface between stream channels and backswamps, may function similarly to hyporheic zones at the interface between aquatic and terrestrial habitats. Within hyporheic zones, intense nitrogen cycling occurs as downwelling of primarily oxygenated surface water into subsurface sediments provides opportunities for aerobic respiration in an otherwise anaerobic environment (Triska et al., 1993). In a riverine wetland, backswamp water may alter stream chemistry as it mixes with river water, and vice versa. These exchange processes depend greatly on the permeability of sediments in the channel's bed and banks, hydraulic gradients, and channel morphology (Malard et al., 2002); therefore, exchange of water and solutes between stream channels and backswamps through a medium of naturally-deposited sediments may be an important factor for nutrient cycling in riverine wetlands.

Preferential flowpaths are widely recognized as mechanisms for rapid subsurface transport of water and solutes (Flury et al., 1994; Sidle et al., 2001; Legout et al., 2009), a process Horton (1933) referred to as "concealed surface runoff." Roots, decayed organic matter, and tunnels of burrowing animals form macropores in structured soils that can function as preferential flowpaths (Gish and Jury, 1983; Nobles et al., 2004; Xin et al., 2009). Additionally, depositional sediment layering and shrink-swell clays form fractures that are obvious structural features in field soils (Figure 1) and form

preferential flowpaths in layered soils (Bouma, 1991). It follows that macropore flow through natural levees may be the dominant mechanism of water exchange between wetlands and river channels, but the influence of these transport mechanisms on the rate and magnitude of flow through natural levees is uncertain.

River Channel-Wetland Interface

Natural levees develop as rivers deposit coarse sediments during overbank flow to form ridges adjacent to the channel, and low-lying backswamps form farther away from the channel bed as slow-moving and still water deposits finer sediments such as silts and clays (Fisk, 1947; Fisk, 1944; Frazier, 1967; Tye and Coleman, 1989). During natural levee development, sedimentation patterns are affected by flood magnitude and duration as well as local geomorphology (Filgueira-Rivera et al., 2007). As the natural levee grows in height, larger flood events are needed to transport coarse sediments over the bank, limiting levee height (Cazanacli and Smith, 1998). Dominant formation processes of fine-grained floodplains include meander belts and associated crevasses and avulsions (Aslan and Autin, 1998)

Figure 1: Exposed bank of a natural levee during low water in the Atchafalaya Basin, Louisiana illustrates structural complexity and potential preferential flow paths.

such that geomorphology is constantly evolving. These processes drive the sedimentation patterns that form and transform river channels, natural levees, and backswamps (Tye and Coleman, 1989).

Floodplain geomorphology often consists of a complex system of stage-dependent surface connections, and natural levees may be an important geomorphic control on surface connectivity (Poole et al, 2002). Where there is extensive surface connectivity, hydraulic gradients across natural levees tend to be ephemeral and small. In riverine wetlands, a specific morphological feature, such as a developing crevasse, may contribute to surface flow patterns to varying degrees at various river stages; thus, hydrology and geomorphology control the surface connectivity between river channels and backswamps or, in the absence of surface connectivity, the magnitude of hydraulic gradients between them.

Hydrologic connectivity in wetlands is important biologically (e.g. Junk et al, 1989) and biogeochemically (e.g. Johnston et al, 2001). Surface connections are likely the dominant mode of connectivity, but subsurface flows may dominate in some floodplains when no surface connect exist (Jung et al 2004). In wetlands such as the Atchafalaya River Basin where surface connections have been reduced (Hupp et al., 2008), ecosystem restoration goals often include re-establishment of surface connections to improve water quality and biogeochemical exchange. However, a lack of information on subsurface connections means that the importance of surface connections relative to total exchange is unknown, and a more complete understanding of natural levee hydrology can improve management planning and efficacy of restoration.

Preferential Flow in Soils

In a low-permeability soil, the majority of mass flux occurs in a small portion of the soil volume via preferential flow paths (Beven and Germann, 1982; Wilson and Luxmoore, 1988). Mechanisms of preferential flow include macropore flow through a network of large holes or fissures (Luxmoore and Ferrand, 1993) and fingered flow through paths formed by discrete currents in the soil matrix (Hillel and Baker, 1988). These preferential flow paths allow event or “new” water, such as rain water, to bypass less-permeable portions of the soil, thus retaining chemical characteristics that differentiate it

from pre-event or "old" water. Identification of old and new water has been used extensively in recent years to investigate mechanisms of stormflow runoff, including preferential flow, in field soils (Buttle, 1994; Luxmoore and Ferrand, 1993; Sklash et al., 1996).

Recently, mechanisms of preferential flow have been reported in wetlands. Harvey and Nuttle (1995) demonstrated that downward infiltration fluxes and upward evaporation-driven fluxes were segregated between macropores and matrix pores respectively in a tidally-influenced riverine wetland in the Virginia coastal plain, and Fitzgerald et al. (2003) found that groundwater seepage to a headwater swamp in a British Columbia rainforest during storm events is dominated by macropore flow. Results from other recent studies of subsurface flow in wetlands suggest that preferential flow is an important mechanism of solute transport (Elci and Molz, 2009; Parsons et al., 2004), but no study to date has specifically investigated the significance of preferential flow in the natural levees of riverine wetlands.

An investigation into the mechanisms of water and solute transport through a natural levee or any field soil must consider the proper scale. Estimation of soil hydraulic properties is limited by the area of influence each measurement describes and the difficulty in obtaining representative measurements (Meinzer, 1932 (reprint 1959)). In this study, characterizing variability at the site scale required choosing a sufficient volume of natural levee to contain features of interest including macropores and other preferential pathways, but upscaling hydraulic properties of field soils to a landscape scale is an emerging science (Kabat et al., 1997; Vereecken et al., 2007). In general, larger scales include more variability, so that hydraulic properties are dependent upon the scale at which they are measured (Seyfried, 1995). This is especially true for preferential flow, which may be dominated by infrequent, large pores (Noguchi, 1999). Therefore, it is critical for field studies to encompass a large enough scale to capture the variability of interest.

Quantifying Solute Transport

Conceptually, solutes may be thought of as moving between two points in a field soil via a set of individual flowpaths. These flowpaths are commonly grouped into two categories, a relatively

mobile domain and a relatively immobile domain, to form a dual-porosity (Gerke and Van Genuchten, 1993) or dual-domain (Liu et al., 2007) conceptual model. In the mobile domain, preferential flowpaths allow rapid solute transport, primarily via advection, to bypass the majority of the soil mass. Solutes moving along flowpaths within the immobile domain experience advective flow at velocities several orders of magnitude slower than in the mobile domain, so Fickian diffusion and hydrodynamic dispersion are more important in determining the rate of solute transport.

The time a solute spends traveling along an individual flowpath is its residence time, and the set of residence times for all flowpaths between two points makes up a residence time distribution (McGuire et al., 2002). The residence time distribution of solutes within natural levees is important for two reasons. Firstly, the timescale of water and chemical transport in the subsurface sediments of riverine wetlands directly relates to nutrient cycling and rates of contaminant conveyance. Faster turnover times of water in the subsurface may provide more dissolved oxygen which affects biogeochemical processes important to water quality (Grimm and Fisher, 1984). Secondly, analysis of residence time distributions allows for inferences of dominant flow mechanisms within natural levee sediments. Because an individual molecule of solute may take one of many possible flowpaths, the solute concentration of water at the receiving point changes through time in part as a function of the residence time distribution.

The concentration of solute measured at a point over time is also known as a breakthrough curve, where the peak of the curve identifies the advective front, and the "head" and "tail" of the curve represent dispersional and diffusional processes on either side of that front. The ratio of advection to dispersion, commonly referred to as the Peclet number, determines the shape of the breakthrough curve (Figure 2). Residence time distributions dominated by advective flow through, for example, continuous macropores, have large Peclet numbers and breakthrough curves with distinct, high-concentration peaks (Figure 2D). At smaller Peclet numbers, the distribution is more damped and has a larger tail, because dispersion increases the proportion of tracer that takes slower pathways (Figures 2A-C). For a given mean flowpath length, the thicker the tail of the breakthrough curve, the

longer the mean residence time of solute in the soil; conversely, a thinner tail with a pronounced peak indicates shorter mean residence times.

The mean of a residence time distribution, mean residence time (MRT), approximates the advective front of the breakthrough curve and provides a useful first order description of the distribution. To calculate MRT from an experimental breakthrough curve, it is helpful to use a well-known statistical distribution as a model of RTD, and a linear system model is a common approach (Jury, 1982). In linear systems theory, an input to a system is related to the response by a transfer function; the most familiar application of this approach in hydrology is instantaneous unit hydrograph theory, in which the input to a watershed is rainfall, the output is streamflow, and the transfer function is the effect of the watershed on the routing of water to its outlet (Dooge, 1973). By using linear systems theory to model residence time distributions of a chemical tracer at various points within a

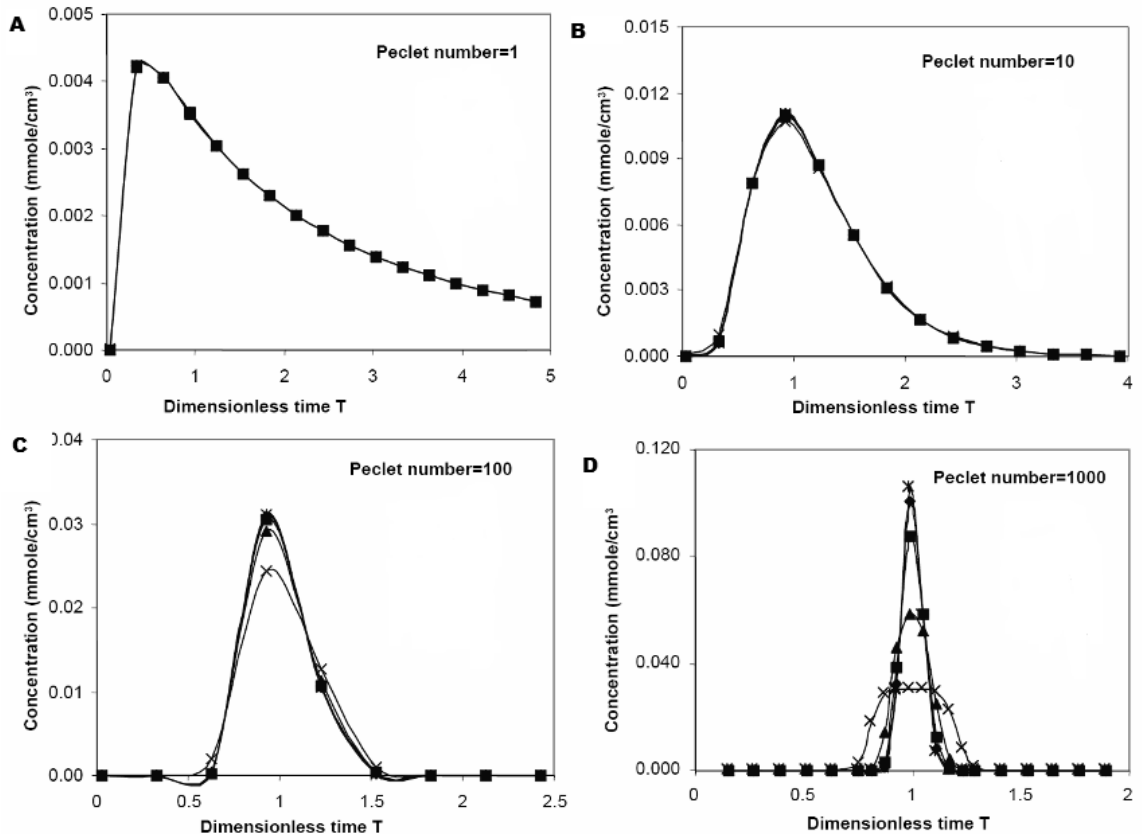

Figure 2: Breakthrough curves represent the probablility distribution of solute residence time based on different Peclet numbers (Wang, 2002).

natural levee, we can calculate MRTs, quantify the spatial variability of transport times, and infer mechanisms contributing to the spatial variability, including the influence of preferential flowpaths. This approach has been used to model a variety of systems, including residence time distributions of isotope tracers in a forested catchment (McGuire et al., 2002) and rain throughfall rates in forest canopies (Keim and Skaugset, 2004).

In a solute transport application under a spatially uniform flow rate, the probability that a tracer will travel distance L after a net amount of water I has been introduced to the system is

$$P_L(I) = \int_0^I g_L(I')\, dI', \tag{1}$$

where $g_L(I')$ is a probability density function, or transfer function, and $I' = I + dI$ (Jury, 1982). In a simple linear system (Dooge 1973), convolving input $x(I)$ with g yields overall response $y(I)$ as a superposition of the individual responses to all units of input I',

$$y(I) = x(I) * g(I') = \int_0^I x(I)g(I')dI'. \tag{2}$$

As such, the convolution involves a "displacement and folding back about the origin" of the input for all I' and integration of its product with the transfer function from zero to I (Hall and Moench, 1972). In field applications, measurements are made at discrete intervals, so that equation 2 becomes a summation:

$$y(I) = \sum_{I'=1}^{I} x(I)g(I'). \tag{3}$$

Similarly, the residence time distribution of hydraulic response can be modeled via a transfer function approach. When a groundwater system is hydraulically perturbed by an input of water, the pressure head instantly increases at the origin of the perturbation, and the resulting pressure wave is transmitted through the system as a function of the hydraulic gradient. This pressure wave is also known as a kinematic wave, and its velocity provides another measure of transport times and flow

mechanisms in a porous medium (Beven and Germann, 1982). Transfer function modeling of hydraulic response is conceptually similar to chemical response modeling according to equation (3) where the input *x(I)* and response *y(I)* are in terms of hydraulic head, and *I* is time. Because chemical transport in a field soil is more complicated than hydraulic transport, a comparison of mean residence times for both measures of transport at the same point in space provides insight into the spatial variability of flow mechanisms.

Objectives

This study was designed to measure the rate of water and solute exchange between wetlands and river channels via shallow subsurface flow and to conceptually characterize dominant transport mechanisms in natural levee sediments within a riverine wetland. Specifically, we aimed to:

- Measure velocities of tracer and pressure wave transport through a natural levee under an imposed hydraulic gradient,
- Determine the spatial variability of transport rates by comparing RTDs of tracers at discrete spatial points within a natural levee, and
- Infer mechanisms of water and solute transport by examining the spatial variability of residence time distributions within a natural levee.

METHODS

We established an approximately 390 m^2 study site on a natural levee in the Atchafalaya River Basin, a large riverine wetland in Louisiana, USA. The field site consisted of a 300-m^2 reservoir and a 10 m x 9 m grid of monitoring wells on the levee crest installed to a depth of 2 m. Wells were instrumented with water level recorders, electrical conductivity sensors, and chloride-specific electrodes. Experiments included hydraulic perturbation and passive and active tracer tests for both artificial and natural events. Using a simple linear system approach, we analyzed breakthrough curves of tracer and pressure wave transport through the natural levee under imposed hydraulic gradient and modeled responses by optimizing parameters of transfer functions to fit observations.

Field Site

The field site for our study was in the Atchafalaya River Basin, the largest contiguous area of forested swamplands in the United States (4678 km^2)(Demas, 2002). In the past century, anthropogenic alterations have increased Mississippi River flow to the Atchafalaya River Basin, increasing water and sediment volume and altering sedimentation patterns and geomorphology (Fisk, 1952; Smith, 1985). By 1975, aggradation had filled most of the Basin's lakes with lacustrine deltas and swamp deposits (Roberts, 1998). Recently-deposited sediments and altered hydrology have important implications for connectivity and thus for subsurface water and solute exchange in the Basin.

Bayou D'arby, a naturally-formed channel on the western side of the lower Atchafalaya River Basin in St Martin Parish, Louisiana near Lake Fausse Point, is in an area of rapid sediment deposition (13-14 mm/yr) and limited surface connectivity (Hupp, 2000; Hupp et al., 2008).This sub-basin is delineated by channels with high levees and spoil banks, forcing water to flow both in and out at the south end, with flow direction driven by the relative water levels at the confluence with the adjacent canal (Figure 3). We conducted a topographic survey of the field site on16 November 2007. Results indicated that the crest of the natural levee has an elevation of 3.3 m above a local datum defined as

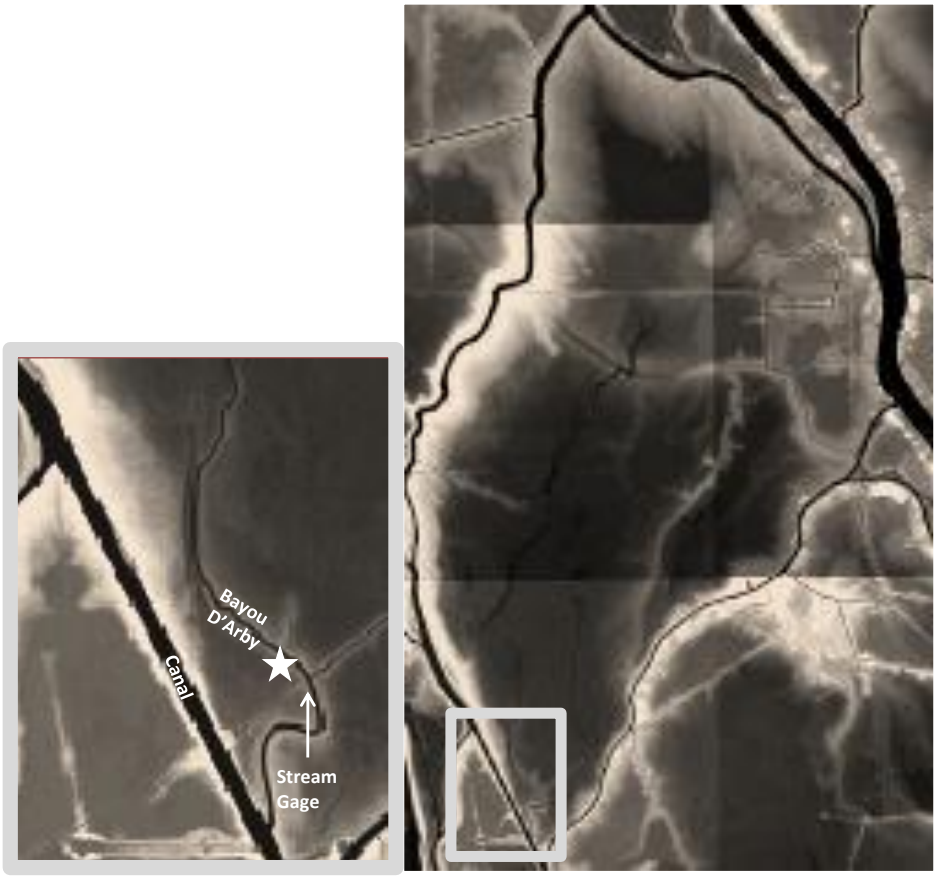

Figure 3: Digital elevation model of Bayou D'Arby sub-basin. Lighter shades of grey indicate higher elevations. Study site (inset) is noted with a star.

the approximate channel bed elevation. The elevation of the natural levee declines into the backswamp to an elevation of 2.4 m above datum, a slope of 0.43 degrees (Figure 4). Water levels and bi-directional flow velocity in Bayou D'arby are monitored by the US Geological Survey at a gage situated on the same reach as our field site (Figure 3). Data indicated that water levels fluctuated during the study period from a high of 3.5-10 m in the spring to a low of 1.5 m in the fall (local datum), indicating that the natural levees are seasonally flooded.

In the Atchafalaya River Basin, soils in the high and intermediate areas on the natural levees range from very fine sandy loams and silty loams, to silty clay loams; lower portions of the natural levees as well as backswamps consist of poorly-drained loamy and clayey soils (Murphy et al., 1977). These soils belong to the Convent soil series which includes a substantial portion of montmorillonitic

(shrink-swell) clays. The strong influence of seasonal wetting and drying cycles on soil formation in the Basin is evidenced by nodules, mottling, and slickensides (Aslan and Autin, 1998). We found little evidence of these indicators, suggesting that soils at our field site are comparatively young.

We analyzed soil samples collected during well excavation at the field site for particle size distribution and soluble salts (all soil tests conducted by the LSU Ag Center Soil Testing and Plant Analysis Lab). Textural analysis indicated a thin upper layer of silt loam underlain by alternating layers of silty clay and silty clay loam and a clay layer beginning at approximately2 m (Figure 4). Soluble salts (obtained by adding 20 g of homogenized soil to 40 ml deionized water, agitating for 30 min, equilibrating for 16 hrs, and measuring EC of the solution) for the first 2 m were between 0.13 and 0.5 ppt but were up to 2.92 ppt at greater depths (Figure 5). Sulfate salts that commonly form in backswamp soils, including those in the Atchafalaya River Basin (Barron, 1996), may be responsible for high salinity. Additionally, our excavations revealed a large unquantified and spatially variable component of organic matter and a root depth of at least two meters.

To measure flow rates and infer dominant flow mechanisms within a large volume of natural levee, we designed a tracer experiment to utilize a 300 m^2 reservoir (Figure 6) as an infiltration zone. When filled, the approximately semi-circular reservoir, constructed on the backswamp side of the levee, provided a hydraulic gradient to drive water through the levee and simulated a natural flood event with ponded water. We constructed the reservoir using sand bags filled with native soil, stacked two to three high to an approximate height of 50 cm, to form a berm on top of the natural soil surface. Plastic sheeting laid over the berm and sealed with packed soil provided insurance against leakage.

A Honda WH15X pump (3.8 L/min) delivered water from the bayou channel into a series of two 0.95 m^3 mixing tanks (Figure 6)which then dispensed the water by gravity into the reservoir. Since we were primarily interested in inferring flow mechanisms from the shape of hydraulic and tracer response curves, estimating mass conservation of tracer was unnecessary, and we monitored water and solute response in only one dimension: from the reservoir through the shallow sediments toward the bayou channel.

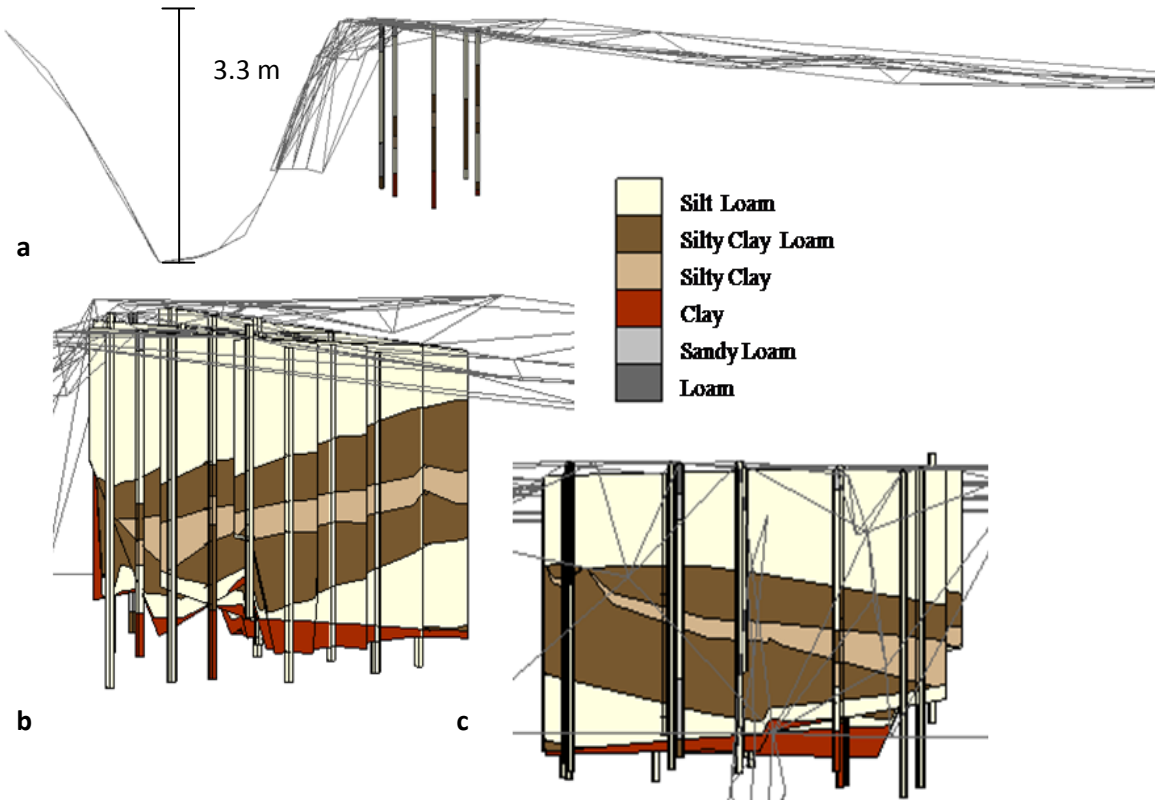

Figure 4: **a)** Side view of research site based on topographic survey measurements; results of soil texture analysis shown. **b)** Interpolation of soil stratigraphy based on soil texture analysis, view from the side and **c)** front.

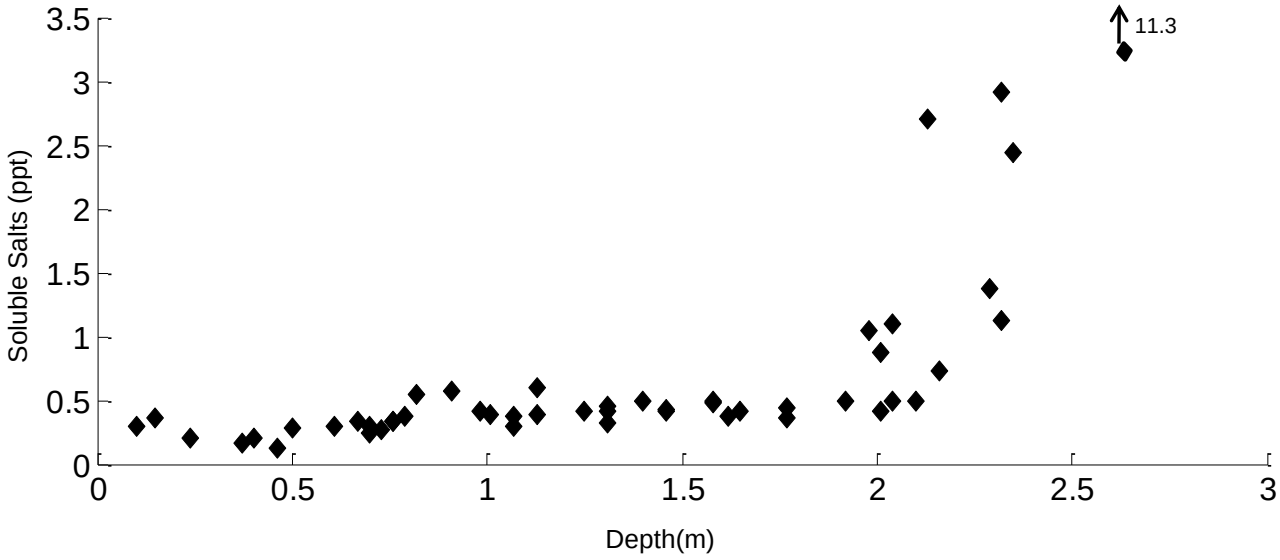

Figure 5: Soluble salts for soil samples collected at the field site.

Figure 6: Left: Reservoir and well field; stream channel is on the left (out of view). Right: Water was pumped into a pair of mixing tanks before being dispensed into the reservoir.

A 10 m x 9 m grid of 18 shallow monitoring wells along the crest of the levee (Figure 7) intercepted lateral flow of water through the shallow sediments. Wells were installed by drilling to the clay layer using a 6.4-cm-diameter hand auger and were screened to 2 m depths. We used two types of well screens to prevent sediment from entering the wells. The first type was constructed from a PVC pipe slotted along its entire length with a table saw and wrapped in nylon stockings. The second type of screen was produced by Atlantic Screen, Inc. Also made of PVC, it was perforated along its entire length with tiny (0.015 cm) slots. Both types of screens were capped at the bottom prior to installation. After inserting the 3.2-cm diameter well screen, the void around the screen was filled with sand for all but the upper 15 cm, and bentonite clay pellets filled the void for the remaining depth to prevent surface water infiltration along the outside of the well.

Instrumentation

Instrumentation of the monitoring wells included four wells with ion-specific electrodes (ISEs) (TempHion 2, Instrumentation Northwest) to measure chloride concentration, electrical conductivity/temperature (EC) sensors (CS547A,Campbell Scientific, Inc.), and Odyssey capacitance water level recorders (3 m long). Three additional wells contained only a conductivity/temperature sensor and a water level recorder. All sensors were programmed to take readings at 3 minute intervals, and the EC and ISE sensors were linked to a central datalogger (CR1000, Campbell Scientific,

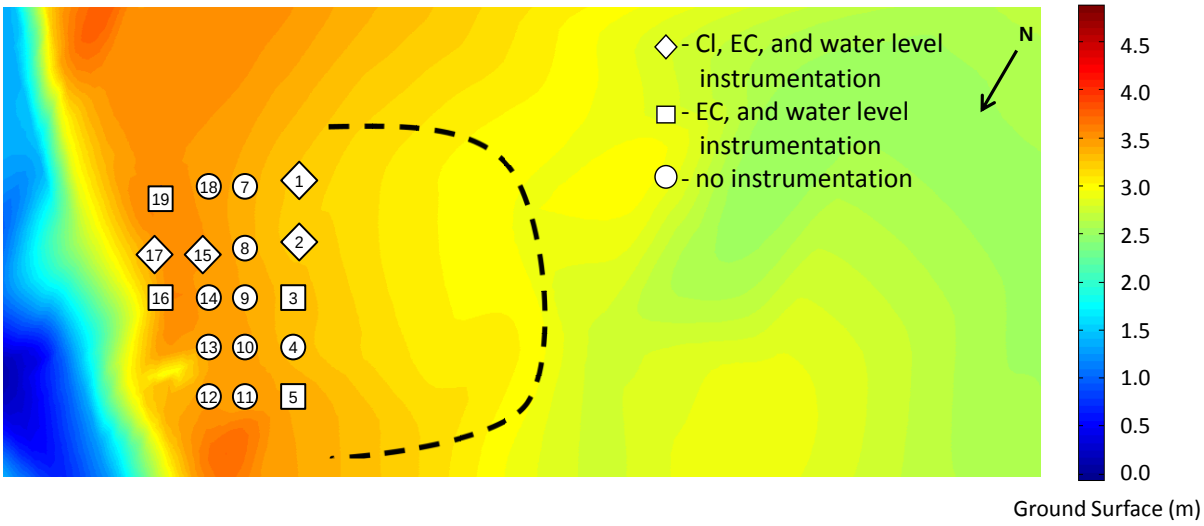

Figure 7: Plan view of site topography (meters above channel bottom) and well layout. Stream channel is on the left, and dashed line indicates approximate reservoir location.

Inc.). Additionally, we manually monitored water levels with a dipper (Model 101,Solinst Mini) and electrical conductivity (EcoSense EC300, YSI Inc.) in the remaining eleven uninstrumented wells throughout each reservoir-filling experiment.

We calibrated the ISEs prior to field deployment according to manufacturer specifications in three different standards (100, 500, and 1000 mg/L Cl^-). Upon initial deployment, the ISEs failed to operate correctly and were returned to the manufacturer for re-plating of the silver-plated electrode. Corrosion of the silver plating may have been related to reducing conditions, but redox of soils at the field site is unknown. Recalibrated ISEs were redeployed on 11 January 2009 and operated through 10 February 2009. The post-deployment calibration check for a 100mg/L solution yielded a range of relative errors: 1.4% (well 2), 5.4% (well 15), 20.4% (well 1), 32.5% (reservoir), and 99.9% (well 17). The data for well 17 indicate that readings began to drift upward (mirroring the behavior of ISEs during initial unsuccessful deployment) several days after the final experiment, so the accuracy of the measurements during the experiments is likely much greater than this post-deployment calibration suggests.

Electrical conductivity sensors were factory-calibrated in a 0.01 molal KCl solution at 25.0˚C. We refined this calibration with a temperature compensation coefficient derived by measuring the EC

of a 1000 mg/L Cl^- solution at room temperature, allowing the solution to warm to ambient temperature, and calculating the temperature compensation coefficient according to manufacturer instructions. A comparison of the pre-deployment and post-deployment measurement of a 1000 mg/L Cl^- solution indicated an average relative error of 10% with a standard deviation of 0.01%. This relative error is double the manufacturer specification (5%) but is reasonable considering field conditions. Because the instruments all behaved similarly during the experiments, the precision of the data is highly reliable.

We calibrated capacitance water level recorders using a two point calibration method per manufacturer specifications. Throughout the data record, there were periodic step shifts of 2-10cm in the apparent water table, with the larger shifts concurrent to instances of data downloading (which necessitated agitation of instruments within the well). The cause of these errors is unknown, but in some instances, it is possible that pressure inside the well was released when the well cap was removed. On 28 January and 2 February 2009 (Experiments 1 and 2), water level in the reservoir was measured with a pressure transducer, and the stream gage measurement for Bayou D'Arby was adjusted to account for the slope between the stream gage and the field site. We determined the slope of the bayou surface by measuring the water level at the field site in relation to the site datum and comparing to the gage reading.

Additionally, a hydrophilic film accumulated on the capacitance cords throughout the course of deployment and affected water level measurements. Post-deployment calibration revealed that film-induced error was proportional to the length of submerged cable. We used this finding in conjunction with manual water table measurements from 28 January 2009 (Experiment 1) to linearly adjust all water levels (Figure 8). These problems affected the accuracy of water level measurements by as much as ±10 cm. However, the precision of the data (ignoring the step shifts) remained intact, and because the primary objective was to measure magnitudes of responses to forcing events, the data are useful for these interpretations. Further analysis of the water levels in relation to one another, the reservoir,

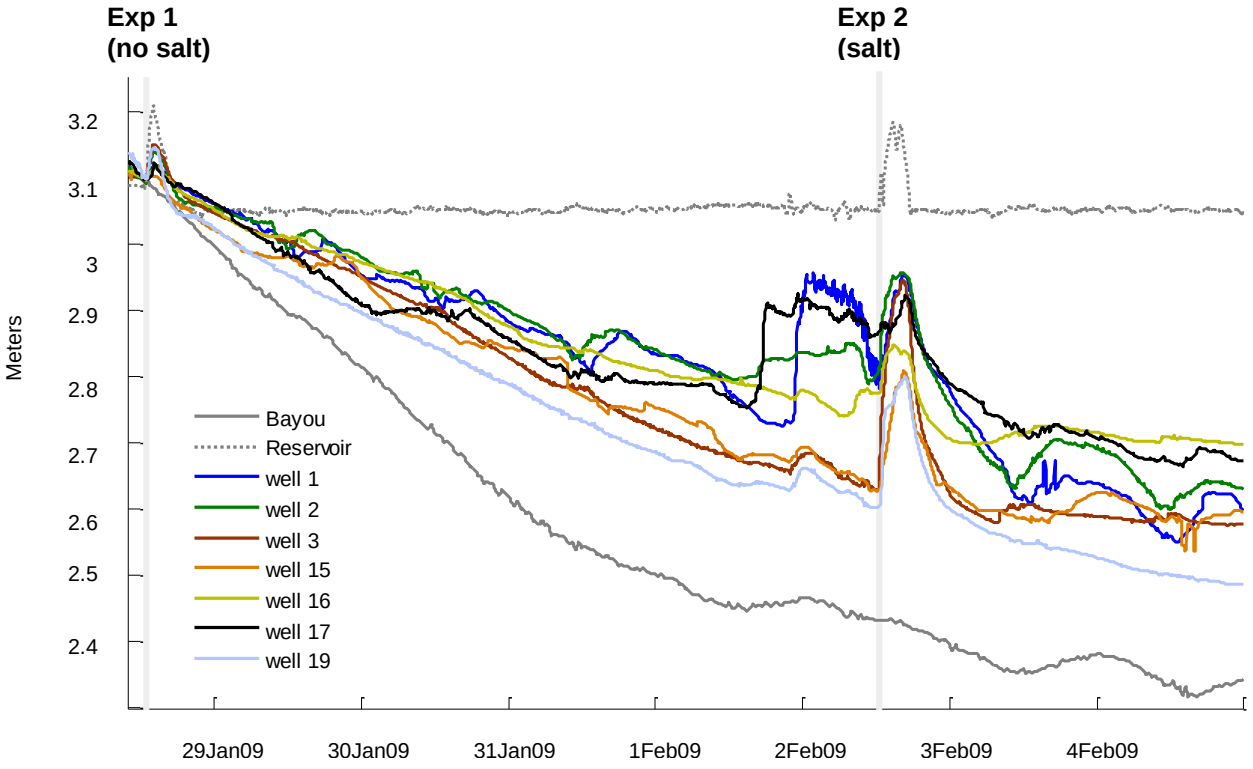

Figure 8: Water levels (in meters from datum, at approximate bayou bed) in wells for experiments 1 and 2, denoted by vertical grey lines. Water levels were corrected to reflect a flat water table immediately prior to experiment 1.

or the bayou is limited by this coarse resolution; although, the reservoir water level (measured with a pressure transducer) for experiments 1 and 2 may be accurately compared to the bayou water level.

Monitored Events and Experiments

We recorded hydraulic and chemical trends for eight forcing events between 1 August 2008 and 10 February 2009 (Table 1). Of these, seven used passive tracers: five pumping events and two intense rain storms (tropical cyclones Faye and Gustav). The remaining pumping event was an active tracer test using potassium chloride (KCl). The water source for passive tracer pumping tests was unadulterated bayou water. Because the natural EC of the bayou water was an order of magnitude lower than the EC of soil pore water, the low-EC water was a natural tracer of event water. We also captured chemical and hydraulic response to two tropical cyclones (storms 1 and 2), providing an

Table 1: Summary of experiments; n/m indicates a variable not measured.

Event	Date	Tracer			Event
		Type	EC (mS/cm)	Cl (mg/L)	
Pump 1	19Aug08	Passive	0.315	n/m	Intermittent pumping following flooding
Storm 1	24-25Aug08	Passive	n/m	n/m	Tropical Storm Faye; 69 mm precip
Storm 2	1-3Sep08	Passive	n/m	n/m	Hurricane Gustav; 415 mm precip
Pump 2	25Sep08	Passive	0.714	n/m	Intermittent pumping
Pump 3	5Nov08	Passive	0.597	n/m	Pumping under dry, low water conditions
Pump 4	5Dec08	Passive	0.709	n/m	Intermittent pumping
Experiment 1 (Exp 1)	28Jan09	Passive	0.315	55	Passive tracer test; short duration pumping with high water table
Experiment 2 (Exp 2)	2Feb09	Active	6	1000	Active tracer test

additional type of passive tracer test. For the active tracer test, we added technical grade (>95% purity) KCl to the mixing tanks to a chloride concentration of roughly 1000 ppm before delivering the solution to the reservoir.

All but the last two events (Experiments 1 and 2) lacked a quantified system input for modeling purposes. Because events “Pump 1”, “Pump 2”, and “Pump 4” were coincident to mechanical and hydraulic troubleshooting and set-up, they were generally intermittent and of short duration but were useful for cursory comparisons of spatial and temporal patterns. Event “Pump 3,” which occurred during dry, low water conditions, was the first intentional experiment. We pumped bayou water continuously into the reservoir for 4.5 hours, but due to very dry conditions, surface ponding did not occur until after approximately 3 hours of mostly-continuous pumping. The instrument recording hydraulic data in the reservoir malfunctioned, so modeling of this event was not possible. Events “Storm 1” and “Storm 2” were tropical cyclones; we used radar-rainfall data from the National

Weather Service online database to estimate precipitation at the field site, but chemical composition of rainfall was unknown.

Events "Exp 1" and "Exp 2" were the only pumping events with quantified system inputs, both hydraulic and chemical, so these are the only events to which we applied a linear system model. High water in the Atchafalaya Basin resulted in flooding of the field site for much of January 2009. On 28 January 2009, just after water levels had sufficiently receded, we pumped bayou water into the reservoir for approximately one hour. When the experiment began, there were already 3 cm of backswamp water in the back of the reservoir, and pumping added 12 cm of hydraulic head. On 2 Feb 2009, we pumped a KCl solution into the reservoir for approximately 3.5 hours, including two 40 minute gaps. The maximum hydraulic head added to the reservoir was 12 cm, but the water table at the outset of the experiment was 20-40 cm lower than the ground surface, so the effective perturbation was on the order of 30-50 cm. Although our intention was to maintain a steady chloride concentration of approximately 1000 mg/L in the reservoir, the solution fluctuated throughout pumping between 800 and 1300 mg/L. The electrical conductivity of the solution fluctuated accordingly: between 4.5 and 6.5 mS/cm. The day before the experiment, a rain event had induced an irregular hydraulic response across the well field, and at the start of this experiment, water levels varied among wells by more than 20 cm (Figure 8).

Modeling

Precipitation events, wind and lunar tides, and differential diurnal evapotranspiration caused perpetual fluctuations in the bayou and shallow groundwater, so a hydraulic gradient always existed across the levee. Modeling the hydraulic response of each well to a forcing event required separating the imposed hydraulic differential from the baseline rising or receding behavior of the water table. We estimated the hydraulic head above baseline using a method comparable to baseflow hydrograph separation, which is commonly used to characterize stream flow response to precipitation (Hewlett, 1982; Lin et al., 2007). To determine the hydraulic baseline, we manually fitted a curve for each well and each event (Figure 9) to approximate the behavior of the water table as it would have been in the

absence of perturbation. First- or second-degree polynomials fitted to data before and after each event provided practical baselines. We then used the point of departure from and return to the hydraulic baseline to define hydraulic response in a specific well.

Hydraulic input and response functions were treated uniformly for both modeled events. Input was defined as the water level in the reservoir above a set datum at the rear of the reservoir, regardless of initial water table condition. For experiment 1, we modified the input to account for the existing standing water in the reservoir. Water level in the bayou provided a logical surrogate for water level in the backswamp because of surface connectivity at the field site, so input was defined as the amount of hydraulic head added to the bayou water level until the bayou equilibrated with the reservoir datum, at which point input was defined as hydraulic head added to the site datum. Both input and response functions were normalized by expressing each data point as a proportion of the entire hydraulic response above baseline.

As with the water tables, modeling chemical response to each forcing event required defining each chemograph in terms of a baseline. For our experiments, we defined water chemistry changes as the proportion of new water to old water. In this conceptual model, there were two "end members" or sources of water for most events: new water and old water. For both tracers we measured, EC and chloride, concentrations varied across the well field at the outset of each experiment by up to 0.6 mS/cm and 200 mg/L respectively, and we interpreted these differences as spatially-variable water age. New water, which either entered the soil from the reservoir or from previous rainfall or bank overflow events, was defined as the concentration of tracer in the reservoir water for each experiment. Old water was defined according to the maximum across the well field for the period of record, the oldest natural soil water measured. Accordingly, the EC of old water was 2.5 mS/cm and for chloride was 300 mg/L, which approximates the asymptotic maximum. This corresponds to approximately 2.5 ppt salinity, which is in the range of soluble salts in the lower part of the soil profile (Figure 5).

Electrical conductivity (1-2.5 mS/cm) and chloride concentration (50-300 mg/L) of the soil solution was generally higher than in surface water (0.3-0.7 mS/cm and 30-55 mg/L, respectively).

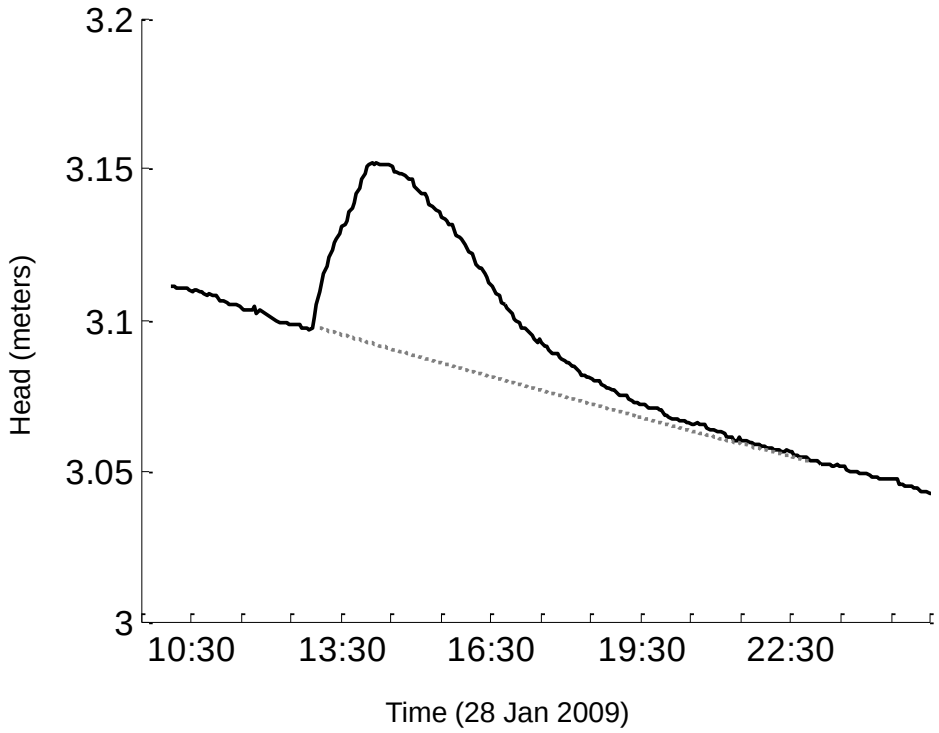

Figure 9: An example hydraulic baseline (dotted line) approximated well response (solid line) in the absence of perturbation (well 3, Exp 1).

Swamp soils are high in soluble salts (Figure 5) because of either evaporative or oxidative precipitation of nutrients (Barron, 1996); longer residence times allow more contact time with the high salinity matrix and result in higher concentrations of solutes (Luxmoore and Ferrand, 1993).

The modeling for the active tracer test (Exp 2) was more complicated than other events; old and new water maintained their previous definitions, but the active tracer provided a third end member. Consequently, the concentration of tracer during the active tracer event in a well at a given time was the result of mixing among three components: old water, new water (containing the active tracer), and bayou water. For simplification, we used an end member mixing analysis (EMMA) technique (Hooper, 1990) to analyze the controlling end members and reduce the effective number of water sources from three to two. In this study, the two tracers were essentially collinear (Figure 10), so discerning between old water and new water (active tracer) response was impossible when

concentrations were between those of bayou water and soil water. Therefore, we defined the old water component for this experiment according to local chemistry at each well.

Modeling tracer according to equation 3 required an estimate of flow through the system. Our experimental design, however, did not conserve mass of water or tracer, so we used the hydraulic head differential between the reservoir and the bayou as a surrogate for flow. We then modeled chemical response as the proportion of new water as a function of cumulative hydraulic head differential between the reservoir and bayou instead of as a function of cumulative flow. We calculated the cumulative hydraulic head differential by summing the "mass" of head differential at each time step. By multiplying cumulative head differential by the time step (three minutes), we obtained "head differential time," which is the time vector weighted or warped by the rate of accumulated hydraulic head. In head differential time, the mean residence times (MRT) of the fitted distributions are in units of m · min (head differential · time); dividing by the approximate average head differential during the experiment (0.12 m for Experiment 1 and 0.7 m for Experiment 2) and estimated pathlengths (Table

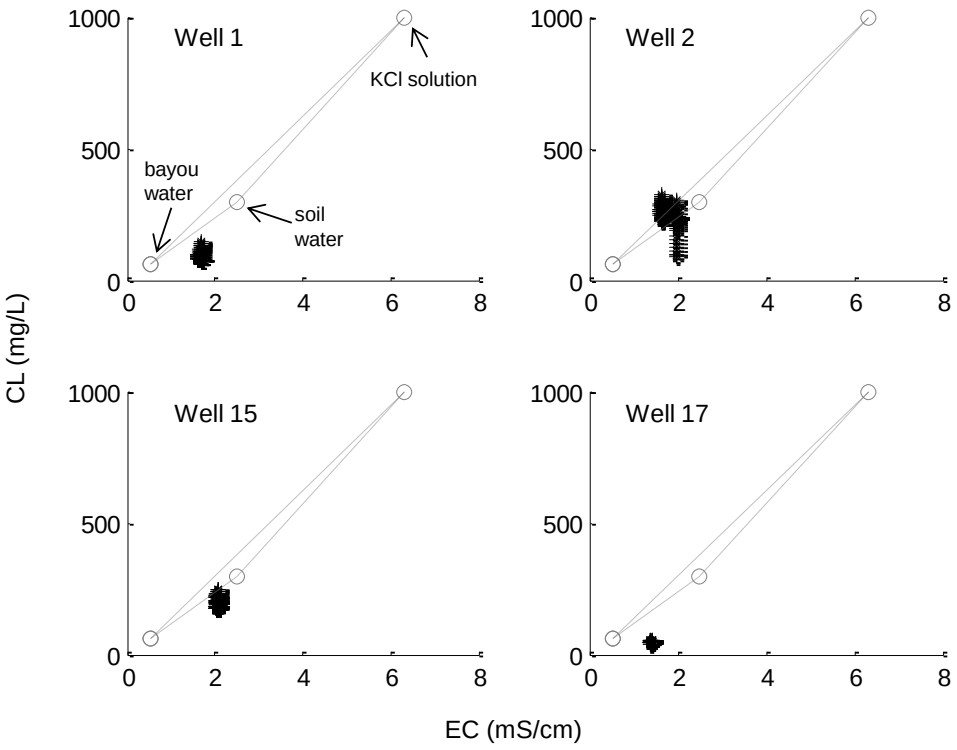

Figure 10: Well chemistry measurements (+) and end members (o) for Exp 2.

2) yields mean travel time (MTT) in units of time. Breakthrough curves for pressure wave transport were modeled in conventional time rather than head differential time.

Unlike conventional time, head differential time was limited by the duration of imposed hydraulic gradient. Once the reservoir was drained, head differential time stopped, and thus modeling in this space also stopped; therefore, breakthrough curves and fitted transfer functions were truncated at this point. The purpose of modeling was to understand the rate of solute movement though a natural levee under realistic hydraulic gradients, which are small and ephemeral. This information is contained in the rising limb of the breakthrough curve—the short-term response—therefore modeling the recession of the chemical breakthrough curves was not essential to the purpose of this study. However, because chemical input was also truncated at the end of head differential time, the tail of the optimized distribution reflects an instantaneous end to the chemical input. Thus the transfer functions provide predictions of both long and short term chemical response, making them useful for interpretation of flow mechanisms.

Calculating velocities of solute transport within the natural levee required estimating path lengths, but we did not attempt to determine the literal paths of water from the point of infiltration to each well. Water from the holding tanks entered the reservoir on the north side and flowed along the berm, filling the reservoir from the back. At the end of pumping, the water receded in the opposite direction; therefore, the infiltration area in the reservoir changed temporally throughout each experiment. Additionally, infiltration points and tortuosity of flow paths are likely driven by substrate variability and micro-topography (for example, the reservoir contains a stump hole where we observed rapid infiltration). Because there are multiple uncertainties, we used the simplest approach by estimating path lengths as the horizontal, straight-line distance from the approximate areal center of the reservoir to each well (Table 2). For each fitted distribution, we divided estimated path length by the MRT to estimate the velocity distribution.

To obtain parameters of the best-fit transfer function for each modeled hydrograph and chemograph, we fit common transfer functions to the experimental data using a Nelder-Mead

numerical optimization search (Lagarias et al., 1998) within Matlab to obtain parameters to maximize the Nash-Sutcliffe efficiency,

$$\varepsilon = 1 - \frac{\sum_{i=1}^{N}(O_i - P_i)^2}{\sum_{i=1}^{N}(O_i - \overline{O})^2}, \quad (4)$$

(Nash and Sutcliffe, 1970) where O is the observed and P is the predicted value at time (or head differential time) i, and $\overline{O}$ is the mean of all observations. The advantage of using ε instead of the more familiar R^2 is that ε is sensitive to the overall variances of observations and predictions. Values of ε

Table 2: Estimated path lengths from the reservoir to each instrumented well.

Well	Path Length (m)
1	12
2	9
3	6
15	13
16	16
17	16
19	19

range from (-1, 1]; $\varepsilon = 1$ indicates perfect agreement, and $\varepsilon < 0$ indicates that the observed mean $\overline{O}$ is a better predictor of the time series of observations than is the model (Legates and McCabe, 1999).

We used two common statistical distributions as transfer functions, the exponential distribution,

$$g(t) = ae^{-at}, \quad (5)$$

where a is a parameter, and the mean of the distribution is a^{-1}; and the gamma distribution,

$$g(t) = \frac{t^{b-1} \cdot e^{-at}}{a^{-1}b\Gamma(b)}, \quad (6)$$

where a and b are parameters, $\Gamma(\ )$ is the gamma function, and the mean of the distribution is $a^{-1} \cdot b$. The exponential distribution, often used to model solute transport in hydrologic systems (Maloszewski and Zuber, 1998; McGuire et al., 2002), assumes that the outflow is linearly-related to the average or well-mixed behavior of the system (Duffy and Gelhar, 1985). Theoretically, the exponential distribution can be thought of as a series of individual flow paths of varying lengths from zero to infinity that do not intersect. The gamma distribution, an infinite series of exponentials, is more consistent with time-series analysis of rainfall-chloride response, reflecting both long-term and short-term watershed response to rainfall (Kirchner et al., 2001).

In some cases, there was a time delay between the hydraulic rise in the reservoir (and concurrent chemical input) and the well response. To account for the time delay, we added a parameter (d) to each distribution that shifted the transfer function in time (or head differential time). In practice, when the delay parameter approached zero, the modeling program produced an error, and the data was modeled without the added parameter. We optimized the delay parameter for each model fit, and the transfer function was defined as:

$$g(t + d). \tag{7}$$

RESULTS

At the outset of this study, we anticipated conducting tracer tests when the hydraulic gradient between the backswamp and bayou was essentially flat, so that the introduced gradient would account for all chemical flux. In reality, water levels within the natural levee sediments were in a perpetual state of change, usually rising in response to rainfall or rising water levels in Bayou D'Arby and dropping as the flood pulse receded; however, the water table never dropped below approximately 2.2 m, near the elevation of the clay layer, though the bayou dropped as low as 1.4 m (Figure 11). Rain events caused short-duration spikes in the water table. Even during periods of relative stillness, there were diurnal fluctuations in the shallow water table, and soil water chemodynamics were in a state of constant flux (Figure 12). Evidence of daily evaporative and tidal fluctuations was apparent in the Bayou D'Arby gage (particularly at low stages) and was reflected in subsurface water levels. Electrical conductivity of the bayou, a product of dynamic flow rates and water sources, also varied widely over the course of the study (Figure 13).

Throughout the monitoring period, subsurface water levels varied spatially by as much as 50 cm, and rather than damping these differences, water added to the system through rain or reservoir-filling events generally maintained or augmented them. Because of instrumentation problems, we were unable to resolve capacitance water level data to a resolution that would allow complete analysis of variation within the water table. However, manual measurements taken before and during experiment 1 illustrate spatially-variable water table response within an uneven water table surface (Figure 14). Immediately before pumping began, water levels varied among wells by 2-3 cm, and as water levels increased in response to pumping, spatial differences persisted. Within a few days, capacitance water level recorders, corrected to reflect a flat water table prior to experiment 1, recorded a 20 cm range of water levels; a rain event then increased the range to approximately 40 cm (Figure 8).

Overall, hydraulic response to forcing events, whether from rain or reservoir-filling, was rapid in all wells, but the magnitude of hydraulic response varied spatially by as much as 50 cm among wells

(Tables 3-5). The largest increase came from hurricane Gustav (Storm 2) which raised the water table by 50-70 cm (Figure 15, Storm 2) and caused Bayou D'Arby to rise 110 cm. During this period of intense rainfall, subsurface water levels rose in advance of the bayou, which indicates infiltration from rainfall as the mechanism of hydraulic response as opposed to river overflow or lateral infiltration through the river bank. We observed direct evidence of macropore flow (Figure 16) during the pumping event that occurred just after hurricane Gustav (Pump 2). A 2-way analysis of variance (ANOVA) indicated that the mean of maximum hydraulic responses across all wells and events differed significantly among forcing events but not among wells, so although hydraulic response varied as a function of the magnitude of each forcing event, hydraulic response to individual forcing events was spatially similar (Figure 17).

Electrical conductivity of the natural levee soil water was also variable, both spatially and temporally, but some notable trends emerged. There was a general decline during the period of record in soil water EC in wells nearest the backswamp (1, 2, and 3); however, in wells nearest the bayou (16, 17, and 19), soil water EC was lower when bayou stage was higher (Figure 12), and the soil water EC trend reflected the bayou EC trend (Figures 12 and 13).

Electrical conductivity response to forcing events (Figure 18) varied in both magnitude and direction and in both time and space. Often, EC change measured in a given well moved in one direction (e.g. increased) during part of a forcing event and then shifted direction later (e.g. subsequent decrease), so for simplification, we characterized EC response as the maximum magnitude of departure from the immediate pre-event EC (Tables 3-5). A 2-way analysis of variance (ANOVA) indicated that the observed variance in maximum response was attributable to differences among forcing events but not among wells, and a multiple comparison test (Tukey-Kramer method) indicated that those differences were between hurricane Gustav (Storm 2) and pumping events 1, 3 and 4 (Figure 19). However, both real and absolute EC change correlated poorly to hydrologic response (R^2=0.12 and 0.04, respectively) (Figure 20).

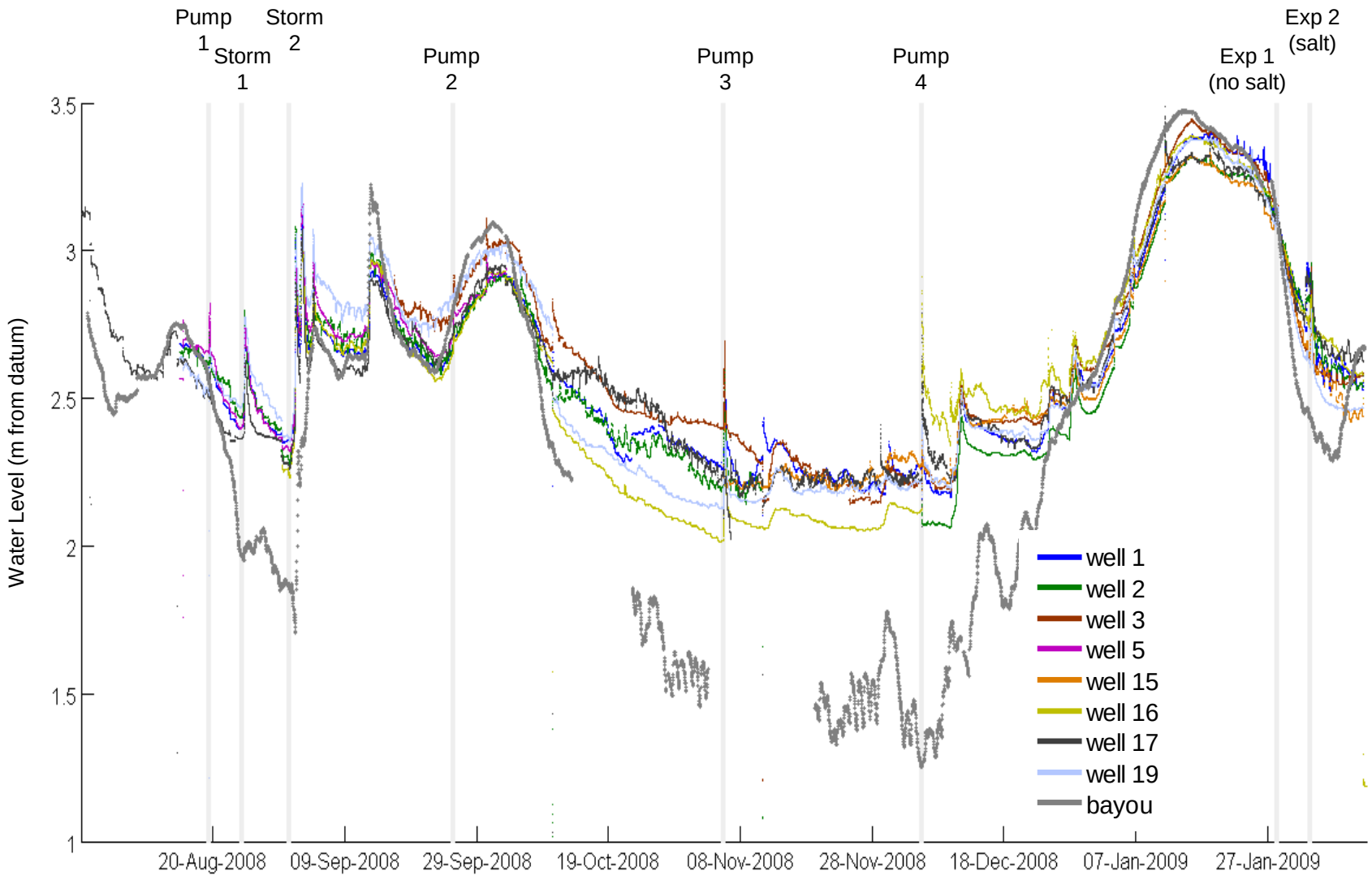

Figure 11: Water level in wells for the period of record. Vertical grey lines indicate individual events.

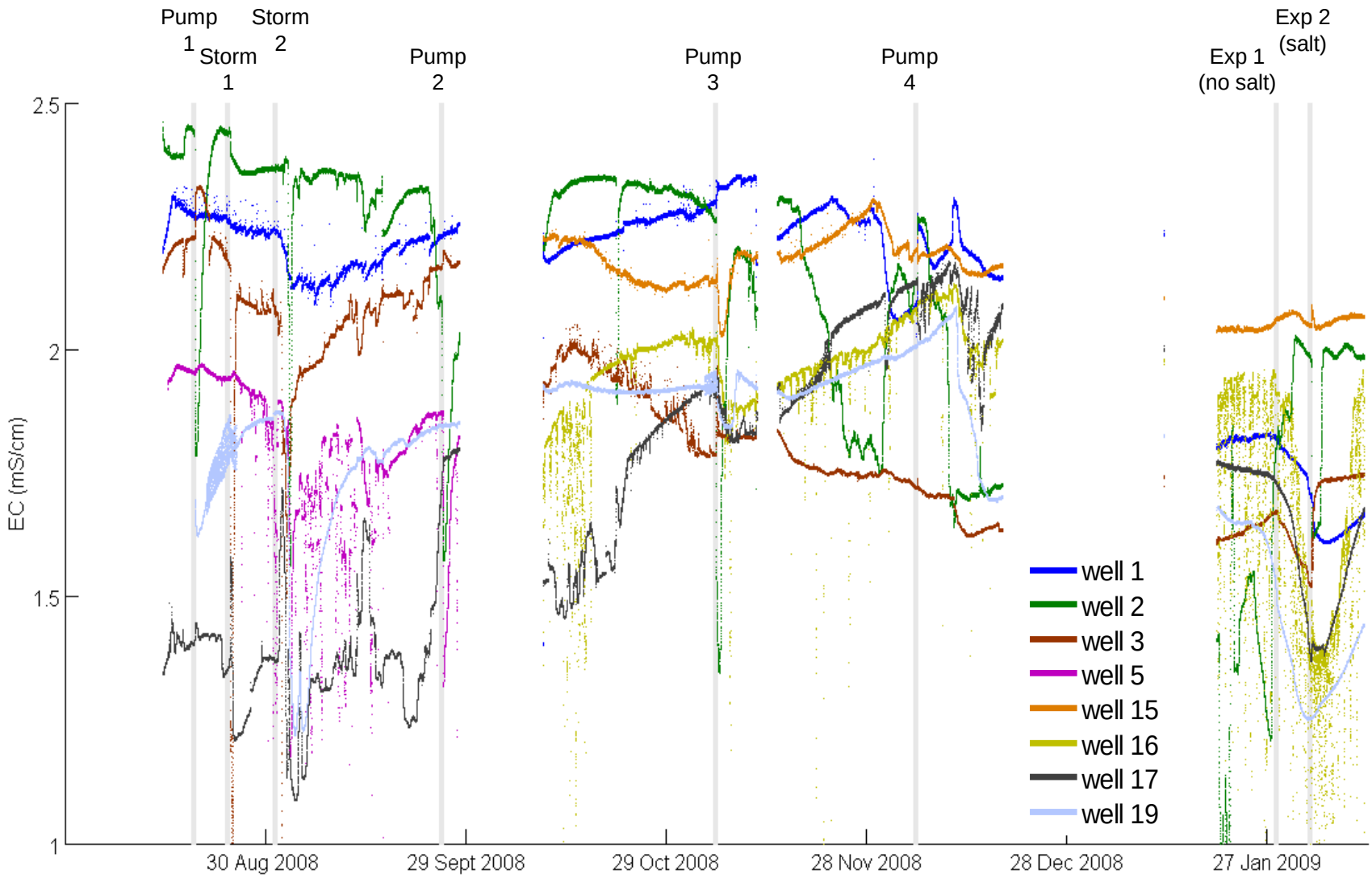

Figure 12: Electrical conductivity in wells for the period of record. Vertical grey lines indicate individual events.

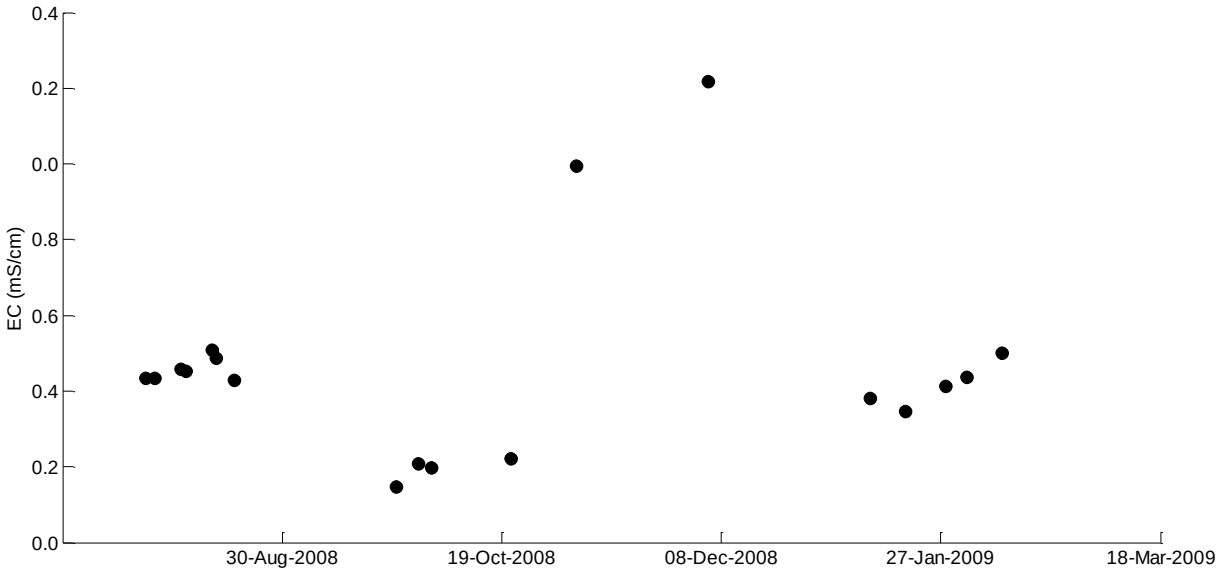

Figure 13: Electrical conductivity of grab samples collected at the field site.

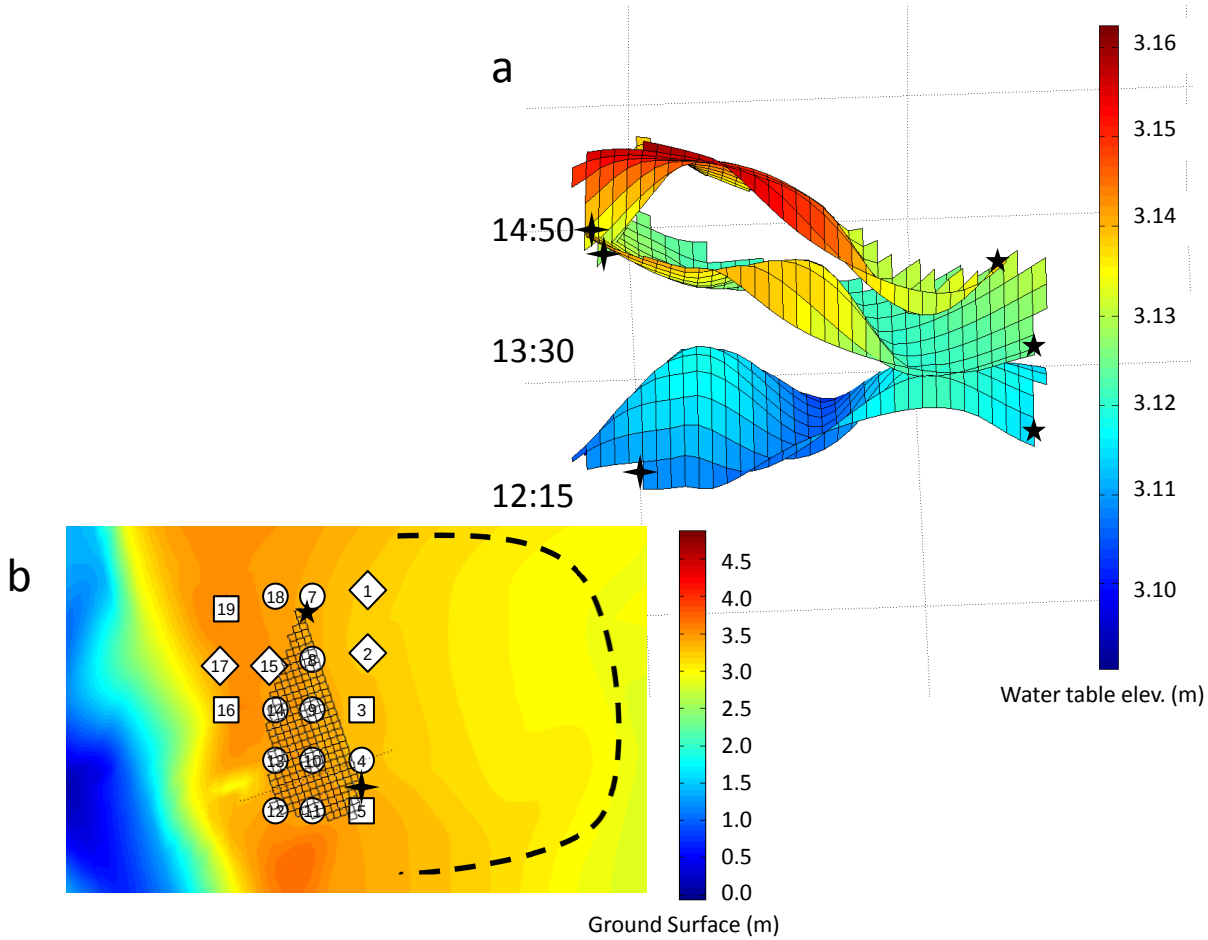

Figure 14: Interpolated water level (a) before (12:15) and during (13:30 and 14:50) experiment 1. Hatched area and corresponding vertices (b) indicate spatial extent of interpolation. X-Y grid is 0.5 m x 0.5 m, vertical scale exaggerated. Refer to Figure 7 for legend of well symbols.

Table 3: Maximum EC and hydraulic response for monitored pumping events; chloride not measured.

Event	Type	Well	Hydraulic Response (cm)	EC Response (mS/cm)
Pump 1	Intermittent pumping after prolonged flooding	1	6	0.00
		2	11	-0.64
		3	--	--
		5	18	0.01
		15	--	--
		16	--	--
		17	10	0.05
		19	9	--
Pump 2	Intermittent pumping	1	5	0.00
		2	6	-0.50
		3	13	0.04
		5	12	-0.56
		15	--	--
		16	6	--
		17	2	0.05
		19	1	0.00
Pump 3	Pumping under dry, low water conditions	1	30	0.05
		2	40	0.93
		3	30	0.19
		5	--	--
		15	--	-0.10
		16	38	-0.20
		17	--	0.01
		19	20	-0.10
Pump 4	Intermittent pumping	1	10	0.20
		2	20	0.16
		3	12	0.10
		5	--	--
		15	10	0.10
		16	66	-0.10
		17	60	0.14
		19	26	0.10

Table 4: Maximum EC and hydraulic response for monitored storm events; chloride not measured.

Event	Type	Well	Hydraulic Response (cm)	EC Response (mS/cm)
Storm 1	Tropical Storm Faye	1	34	0.00
	69 mm precip	2	32	-0.10
		3	30	-1.30
		5	30	0.01
		15	--	--
		16	--	--
		17	29	-0.21
		19	25	--
Storm 2	Hurricane Gustav	1	70	-0.11
	415 mm precip	2	69	-0.82
		3	--	-1.20
		5	65	-0.73
		15	--	--
		16	50	--
		17	65	0.35
		19	64	-0.67

Table 5: Maximum EC, chloride, and hydraulic response for experiments.

Event	Type	Well	Hydraulic Response (cm)	EC Response (mS/cm)	Chloride Response (mg/L)
Exp 1	Pasive tracer experiment	1	3	-0.02	10
	12 cm hydraulic	2	5	0.04	0
	gradient between	3	6	-0.02	--
	reservoir and bayou	5	--	--	--
		15	2	0.00	--
		16	3	--	--
		17	3	0.01	0
		19	6	0.01	0
Exp 2	Active tracer experiment	1	20	0.01	85
	70 cm hydraulic	2	17	-0.35	240
	gradient between	3	32	0.21	--
	reservoir and bayou	5	--	--	--
		15	19	0.05	18
		16	10	0.14	--
		17	8	0.04	9
		19	21	0.00	--

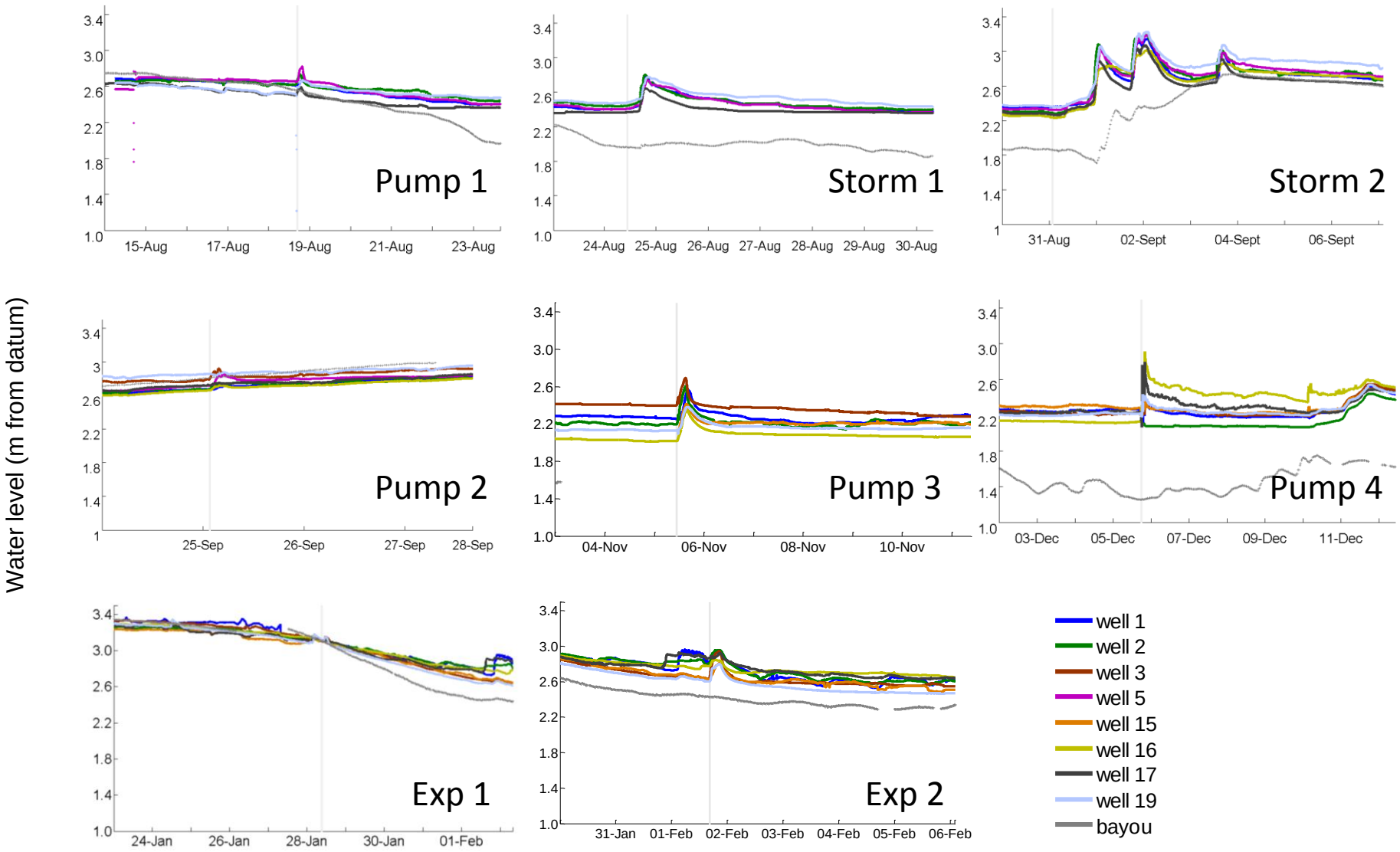

Figure 15: Water level in wells for individual events, indicated by vertical grey line.

Figure 16: Water exfiltrates through a macropore just outside the reservoir during a pumping experiment.

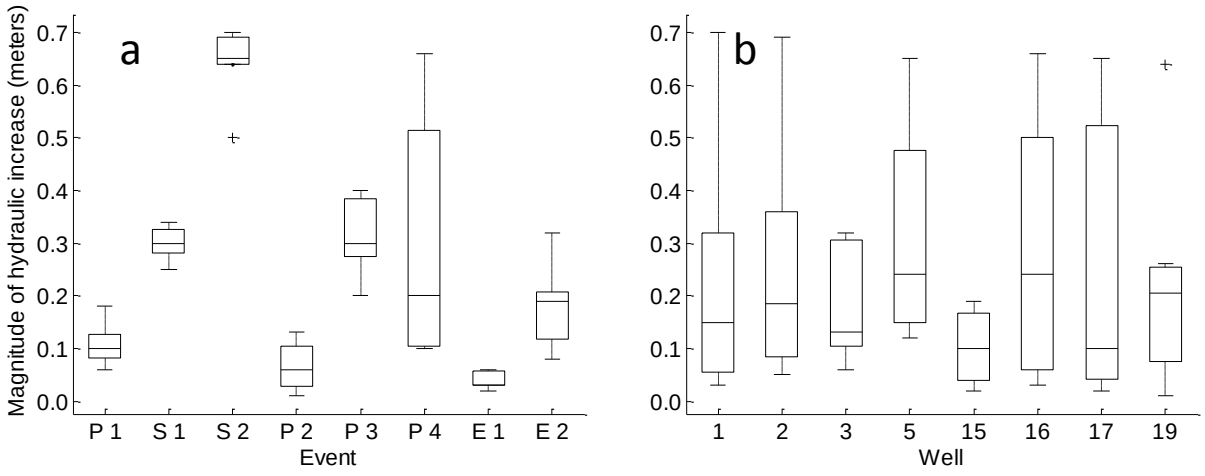

Figure 17: Maximum hydraulic response of wells by event (a) and well (b). Boxplots are marked at the lower quartile, median, and upper quartile values. Whiskers illustrate the range of data with outliers displayed as a plus sign.

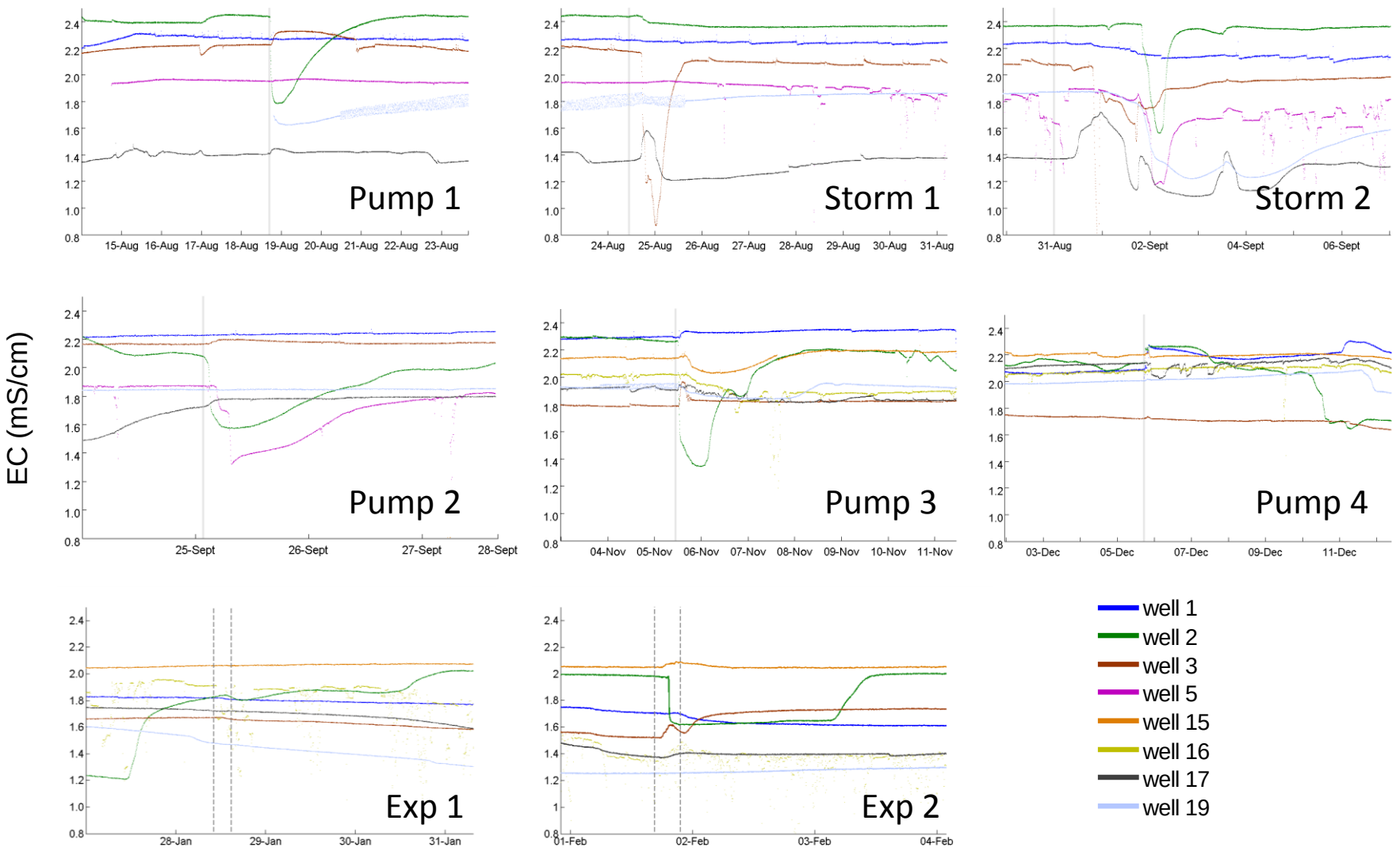

Figure 18: Electrical conductivity in wells for individual events, indicated by vertical grey line. For experiments 1 and 2, dashed lines delineate the modeled period in which reservoir held water.

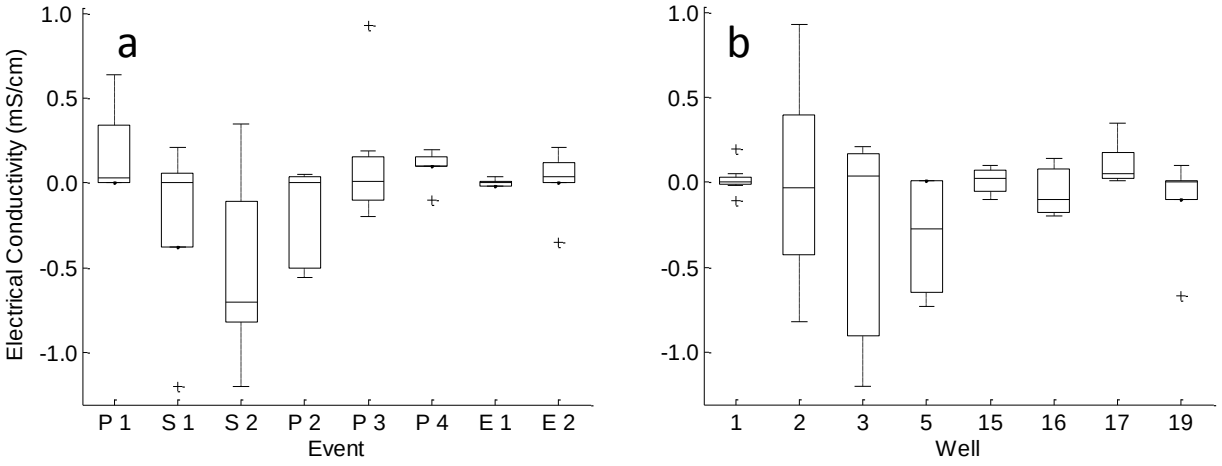

Figure 19: Maximum EC response of wells by event (a) and well (b). Boxplots are marked at the lower quartile, median, and upper quartile values. Whiskers illustrate the range of data with outliers displayed as a plus sign.

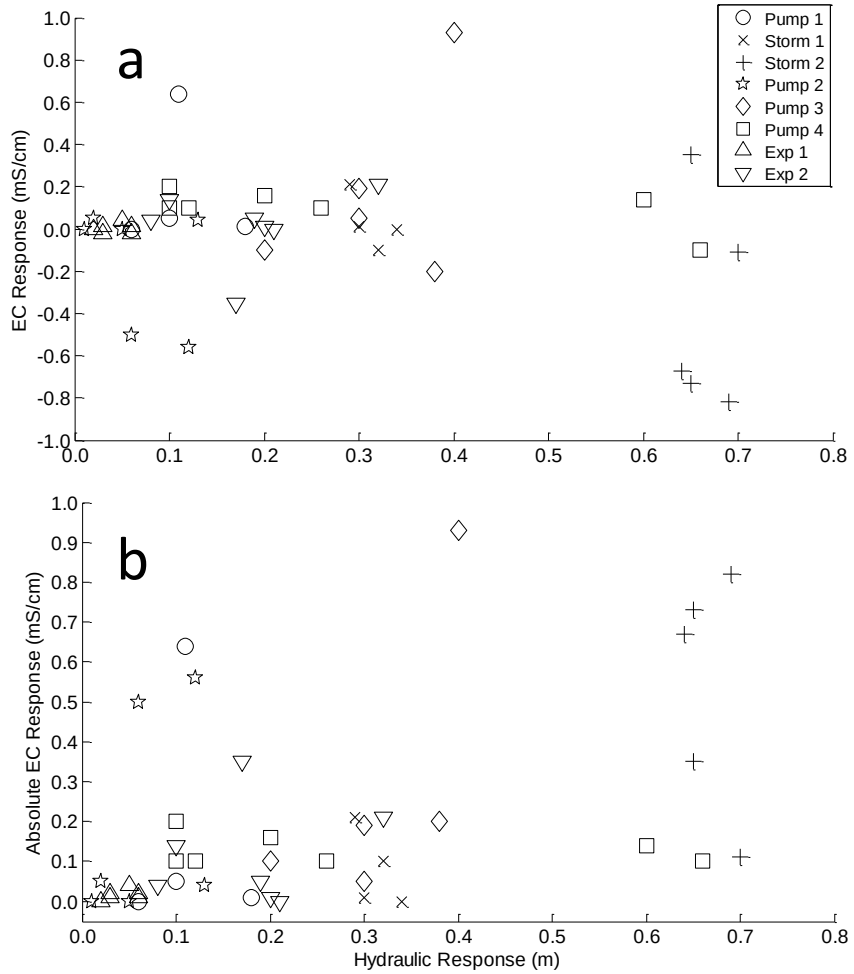

Figure 20: Real (a) and absolute (b) maximum EC and hydraulic response.

We measured chloride concentration only for experiments 1 and 2 (Table 5). In the passive tracer experiment (1), the only discernable short-term change in chloride concentration was in well 2 (Figure 21). Nonetheless, the trend during the period of record suggests that chloride is a dynamic variable in the natural system; an increasing trend of chloride concentration measured in wells 2 and 15 was reversed when bayou water was pumped into the reservoir during the passive tracer experiment, but the trend shift occurred after the period of modeling, once the reservoir had drained. In the active tracer experiment (2), the soil water chloride concentration increased markedly in all instrumented wells. Despite the general collinearity of the two tracers (Figure 22), the direction of the chloride responses was opposite the EC responses in wells 1 and 2.

Residence Time Modeling

Linear system models provided good simulations of the observed pressure wave transport with both exponential and gamma distributions, with a mean Nash-Sutcliffe efficiency (ε) for both events and all wells of 0.93 (range 0.71 – 0.99) (Tables 6 and 7). The proportional mass difference between observed and predicted response reflected discrepancies in curve shape and provided an additional measure of model fit. The grand mean proportional mass difference for all simulations was 4.8 E-3. In all cases, the best-fit time delay was zero. The grand mean MRT for all wells and both events was 74.5 (range 1.4 – 400) minutes, and the grand mean transport velocity was 0.02 (range 5.0 E-4 – 0.23) m/s. Pressure wave transport velocities were faster by an order of magnitude in experiment 1 (mean 0.03 m/s) than in experiment 2 (mean 0.003 m/s).

Overall, linear system models provided good simulations of the observed tracer transport (grand mean 0.64) (Tables 8 and 9). Exceptions were the EC response for wells 2 and 15 in experiment 1 (Figure 23) and the chloride response for well 15 in experiment 2 (Figure 24), which were more complex than the simple conceptual linear model. The proportional difference between the integral of the response curve and the integral of the simulation reflected discrepancies in curve shape and provided an additional measure of model fit (grand mean 0.02), but values may also reflect mass loss from numerical integration.

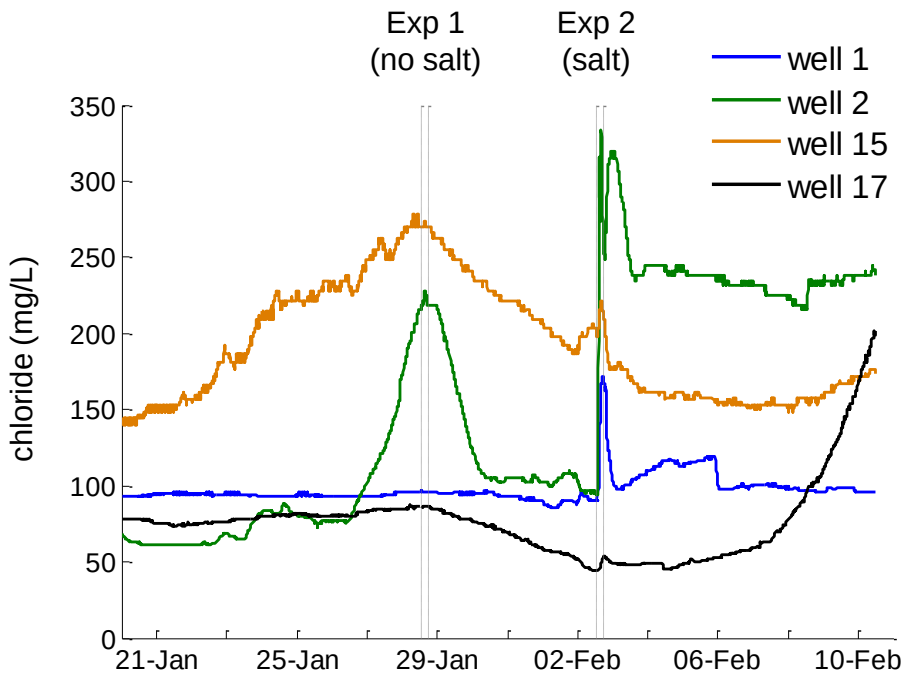

Figure 21: Chloride concentration in wells for the period of record. Vertical lines delineate modeled period in which reservoir held water for individual events.

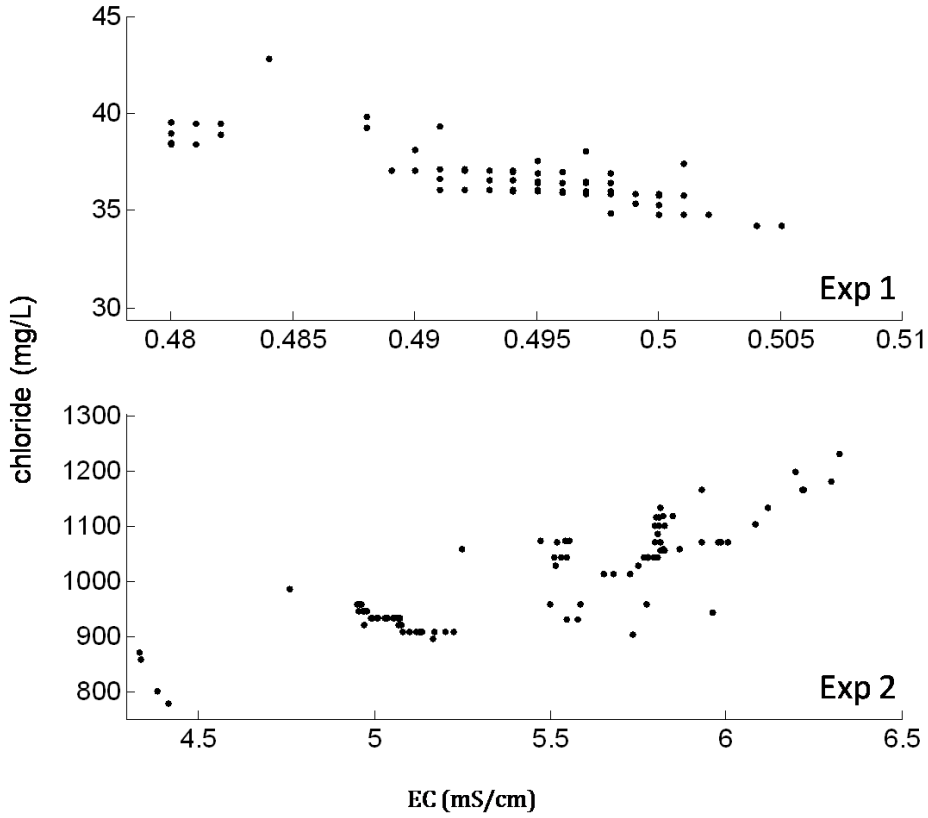

Figure 22: Electrical conductivity and chloride measured in the reservoir during experiments 1 and 2.

Table 6: Modeling results of pressure wave transport for experiment 1. The best-fit value for the time delay parameter *d* is zero for all tests. Negative values of proportional mass difference indicate an over-prediction of mass in the tail of residence time distributions.

				Parameters				
Model	Well	Efficiency (ε)	Proportional Mass Difference	a	b	MRT (min)	Variance	Velocity (m/s)
Exponential	1	0.96	5.6 E-8	0.0312	--	32	1.0 E3	6.2 E-3
	2	0.98	2.7 E-15	0.0721	--	14	1.9 E2	1.1 E-2
	3	0.98	1.2 E-12	0.0603	--	17	2.8 E2	6.0 E-3
	15	0.71	1.3 E-9	0.0396	--	25	6.4 E2	8.6 E-3
	16	0.96	2.9 E-8	0.0325	--	31	9.5 E2	8.7 E-3
	17	0.89	6.3 E-11	0.0467	--	21	4.6 E2	1.2 E-2
	19	0.91	9.9 E-2	0.2755	--	4	1.3 E1	8.7 E-2
Mean		**0.91**	**1.2 E-8**			**21**	**5.1E2**	**2.0 E-2**
Gamma	1	0.98	2.0 E-3	0.0198	0.3206	16	8.2 E2	1.2 E-2
	2	0.98	-1.3 E-6	0.1222	0.5646	5	3.8 E1	3.3 E-2
	3	0.99	9.3 E-4	0.0217	0.1833	8	3.9 E2	1.2 E-2
	15	0.82	5.8 E-2	0.0036	0.1541	43	1.2 E4	5.0 E-3
	16	0.96	1.1 E-5	0.0515	0.5804	11	3.2 E2	2.4 E-2
	17	0.92	7.7 E-15	2.8604	24.86	9	3.0 E0	3.1 E-2
	19	0.91	-9.9 E-7	3.6603	5.068	1	0.38 E-1	2.3 E-1
Mean		**0.94**	**8.7 E-3**			**13**	**1.9 E3**	**4.9 E-2**

Table 7: Modeling results of pressure wave transport for experiment 2. The best-fit value for the time delay parameter *d* is zero for all tests. Negative values of proportional mass difference indicate an over-prediction of mass in the tail of residence time distributions.

				Parameters				
Model	Well	Efficiency (ε)	Proportional Mass Difference	a	b	MRT (min)	Variance	Velocity (m/s)
Exponential	1	0.91	9.8 E-3	0.0025	--	400	1.6 E5	5.0 E-4
	2	0.88	2.0 E-3	0.0043	--	233	5.4 E4	6.5 E-4
	3	0.91	3.2 E-3	0.0075	--	133	1.8 E4	7.5 E-4
	15	0.98	3.1 E-3	0.0060	--	167	2.8 E4	1.3 E-3
	16	0.92	3.0 E-3	0.0085	--	118	1.4 E4	2.3 E-3
	17	0.90	3.0 E-3	0.0075	--	133	1.8 E4	2.0 E-3
	19	0.88	2.9 E-3	0.0061	--	164	2.6 E4	1.9 E-3
Mean		**0.91**	**4.1 E-3**			**192**	**1.5 E4**	**1.3 E-3**
Gamma	1	0.95	2.0 E-2	0.0050	0.7273	145	2.9 E4	1.4 E-3
	2	0.94	7.7 E-3	0.0062	0.5784	93	1.5 E4	1.6 E-3
	3	0.97	3.2 E-3	0.0089	0.4827	54	6.0 E3	1.9 E-3
	15	0.99	3.2 E-3	0.0126	0.7466	59	4.7 E3	3.7 E-3
	16	0.94	2.7 E-3	0.0135	0.5918	44	3.2 E3	6.1 E-3
	17	0.92	5.3 E-4	0.0524	2.1147	40	8.1 E2	6.6 E-3
	19	0.93	8.4 E-3	0.0079	0.5249	66	8.4 E3	4.8 E-3
Mean		**0.95**	**6.6 E-3**			**72**	**9.6 E3**	**2.5E-3**

When water chemistry in instrumented wells differed from our simple conceptual model that a given input would result in a shift toward either old or new water chemistry, the linear system model was not appropriate. In experiment 1, EC in well 17 spiked in the direction of old water but subsequently returned to the pre-event EC during the period of imposed hydraulic gradient (Figure 23), and the only discernable short-term chloride response for experiment 1 (in well 2) similarly shifted from a new-water to old-water response. In experiment 2, the direction of EC response in wells 1 and 3 also shifted during the period of imposed hydraulic gradient (Figure 24). The instrument in well 16 recorded an EC signal that was difficult to distinguish from noise (Figure 18), thus well chemistry was not modeled. The EC response for wells 2 and 15 in experiment 1 (Figure 23) and the chloride response for well 15 in experiment 2 (Figure 25) were more complex than the simple conceptual model but not enough to prevent modeling.

Concentration of tracer in the soil water varied spatially for both experiments, but the variability was greater in experiment 2. The mass difference between the integral of the input and response functions, expressed as a proportional change in new or old water, provided a useful measure of tracer mass recovery (Figure 26). In experiment 1, the proportion of the total recovered tracer mass was distributed approximately evenly among wells; wells 15 and 17 were excluded because proportional change was not measureable. In experiment 2, however, spatially disparate proportional change in soil water chemistry was apparent. For well 2 EC (Figure 26b), the calculation reflects a proportional change in old-water EC rather than directly-recovered tracer mass.

The transport of pressure waves in the subsurface differed from the transport of tracers in both velocity and spatial variability. The mean velocity of pressure waves was faster than the mean velocity of tracers by two orders of magnitude (1.9 E-2 and 4.3 E-4 m/s, respectively), and the mean variance of hydraulic residence time distributions was smaller than the mean variance of tracer RTDs by seven orders of magnitude (1.4 E4 minutes and 7.9 E11 minutes, respectively) (Tables 6 - 9). The majority of optimized pressure wave gamma RTDs had modal residence time probability at t=0 (Figure 27), indicating rapid water table response to hydraulic input. When the shape of parameter *b*

in the gamma distribution equals one, the distribution is exponential, so optimized distributions with *b* near one approximate the exponential distribution. Relative mean residence times for the two experiments indicate that hydraulic head remained in the system longer in experiment 1 (Table 6) than in experiment 2 (Table 7) by an order of magnitude. The higher water table during experiment 1 likely explains why the greater mass arrived at earlier times, because in experiment 2, filling of empty pores in the subsurface probably accounted for some new water and thus damped the effect of the hydraulic input on the pressure wave.

Like the optimized pressure wave RTDs, the majority of optimized tracer RTDs had modal residence time probability at t=0 (Figure 28), indicating rapid chemical response to tracer input, but the overall range and timescale of tracer RTDs was more variable than pressure wave RTDs. The best-fit RTDs for electrical conductivity in well 2 in experiment 1 (Figure 28b) indicated rapid response to tracer input after a delay of approximately 30 minutes. In reality, this best-fit model was obtained because the data did not fit the conceptual model: the water chemistry responded immediately with a decrease in proportion new water before switching to an increase in proportion new water (Figure 23, well 2), but the model only fit the increase. In experiment 2, both chemical tracers were modeled in wells 2, 15, and 17, and residence time distributions for each pair scaled similarly, but the optimized gamma model of chloride for well 17 predicted earlier arrival of the advective front as compared to the optimized gamma model of electrical conductivity (Figure 28d).

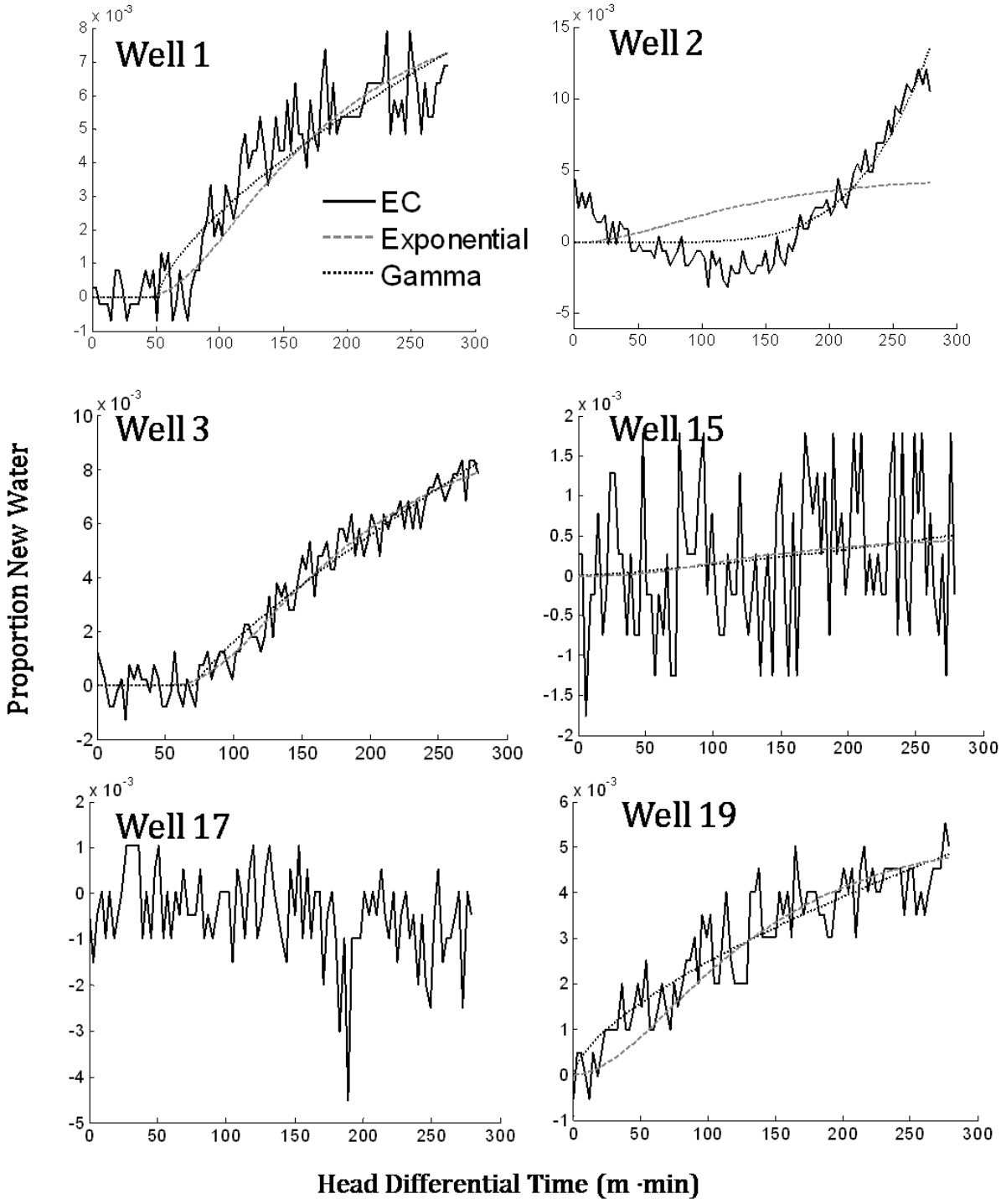

Figure 23: Optimized models of electrical conductivity for experiment 1. EC response in well 17 was not modeled for this event.

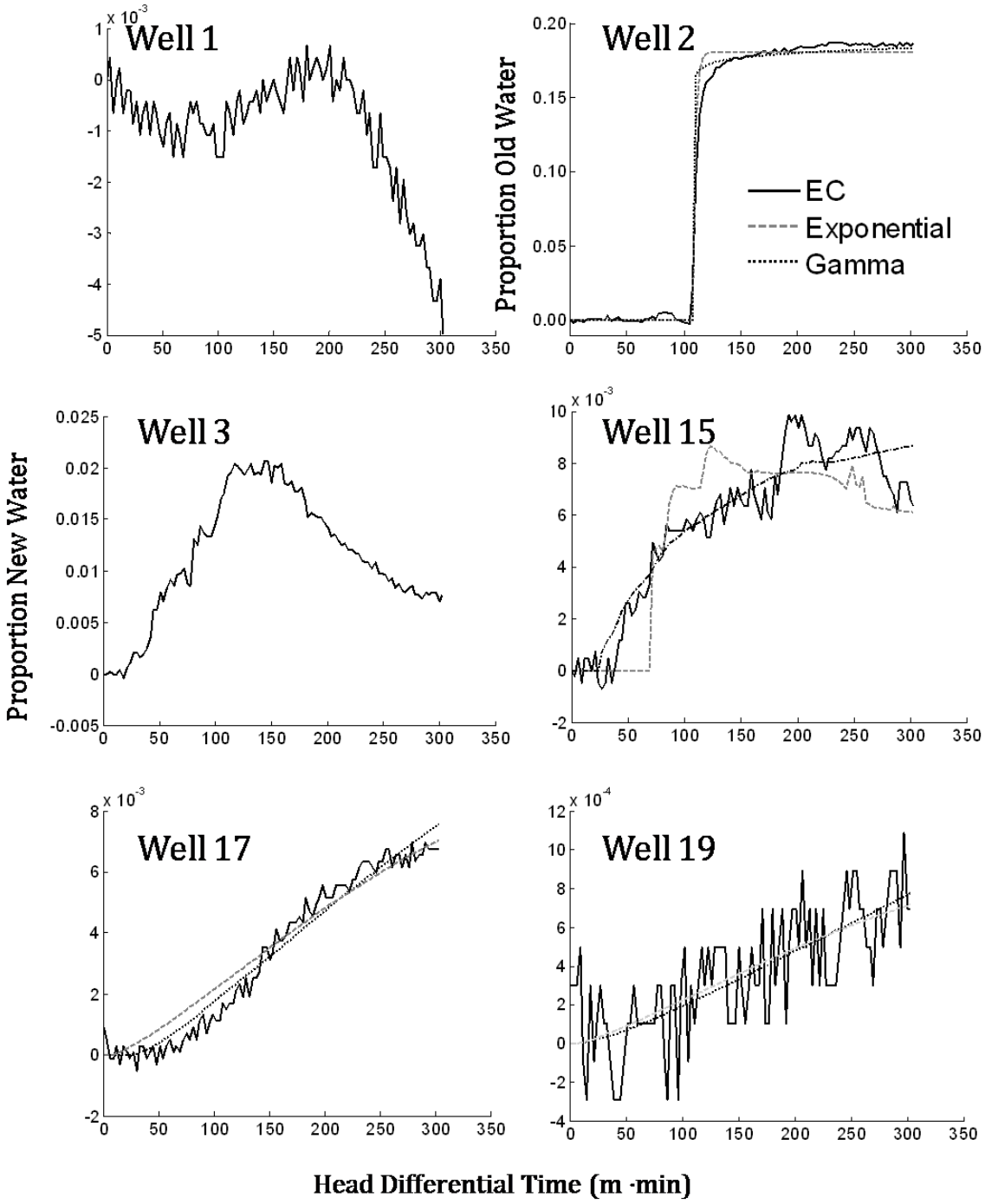

Figure 24: Optimized models of electrical conductivity for experiment 2. EC response in wells 1 and 3 was not modeled for this event. Well 2 was modeled with an inverse input function.

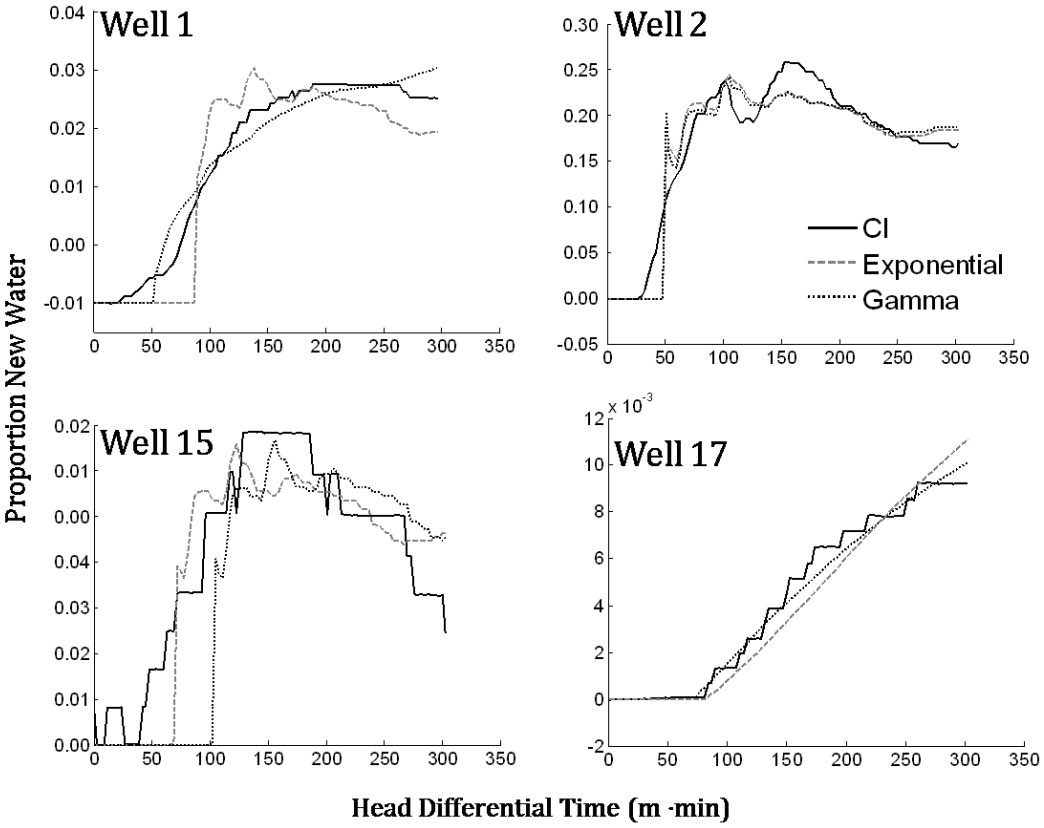

Figure 25: Optimized models of chloride for experiment 2.

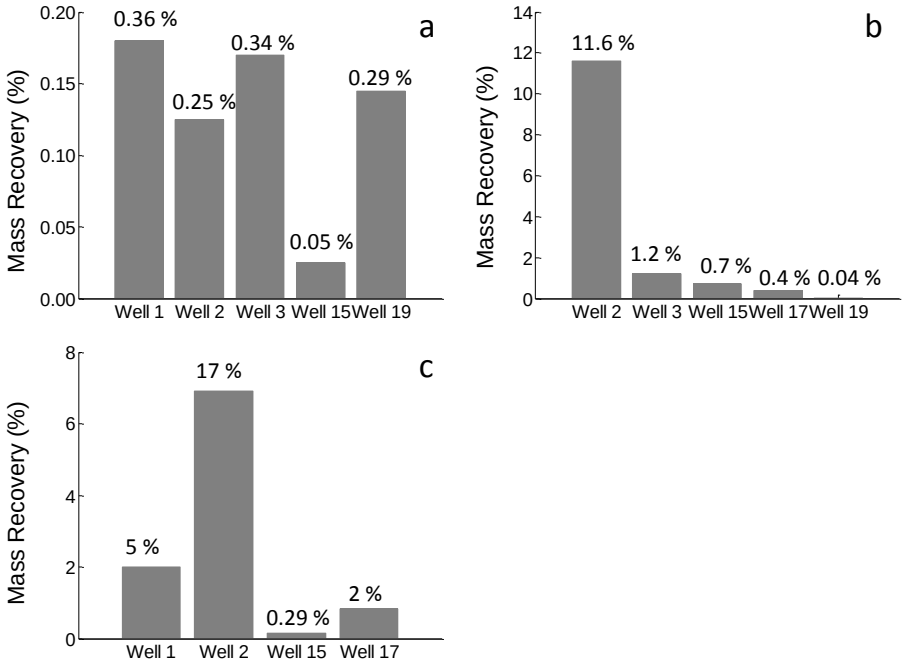

Figure 26: Mass recovery of tracer for experiment 1 EC (a), experiment 2 EC (b), and experiment 2 chloride (c).

Table 8: Modeling results of tracer transport for experiment 1. Negative values of Mass Diff (proportional mass difference) indicate greater mass in the model than in the observations.

					Parameters					
Model	Well	Tracer	ε	Mass Diff	a	b	Delay (min)	MRT (min)	Variance (min)	Velocity (m/s)
Exponential	1	EC	0.86	0.049	2.0 E-4	--	380	4.2 E4	6.7 E10	4.8 E-6
		Cl	--							
	2	EC	0.24	-0.204	1.0 E-4	--	39	8.3 E4	7.9 E4	1.8 E-6
		Cl	--							
	3	EC	0.95	0.008	3.0 E-4	--	500	2.8 E4	4.7 E9	3.5 E-6
	15	EC	0.04	-0.103	1.5 E-5	--	195	5.4 E5	1.2 E10	4.0 E-7
		Cl	--							
	16	EC	--							
	17	EC	--							
		Cl	--							
	19	EC	0.80	0.044	1.6 E-4	--	0	5.1 E4	7.3 E11	6.2 E-6
Mean			**0.55**	**-0.004**			**219**	**1.6 E5**	**1.6 E11**	**2.9 E-6**
Gamma	1	EC	0.87	0.020	9.3 E-6	6.9 E-1	438	6.3 E5	8.8 E8	2.7 E-7
		Cl	--							
	2	EC	0.85	-0.123	2.7 E-2	7.1 E0	32	2.2 E3	8.3 E8	5.7 E-5
		Cl	--							
	3	EC	0.95	0.020	3.8 E-5	8.2 E-1	636	1.8 E5	9.3 E7	5.6 E-7
	15	EC	0.04	-0.083	3.0 E-5	1.3 E0	21	3.5 E5	3.5 E10	5.2 E-7
		Cl	--							
	16	EC	--							
	17	EC	--							
		Cl	--							
	19	EC	0.83	-0.007	3.9 E-5	1.2 E0	24	2.0 E6	2.8 E8	1.3 E-7
Mean			**0.71**	**-0.003**			**230**	**6.3 E5**	**7.5 E9**	**1.4 E-5**

Table 9: Modeling results of tracer transport for experiment 2. Negative values of Mass Diff (proportional mass difference) indicate greater mass in the model than in the observations.

					Parameters					
Model	Well	Tracer	ε	Mass Diff	a	b	Delay (min)	MRT (min)	Variance (min)	Velocity (m/s)
Exponential	1	EC	--							
		Cl	0.85	0.058	6.9 E-1	--	128	1.3 E2	3.0 E0	1.5 E-3
	2	EC	0.99	0.002	4.7 E-1	--	160	1.6 E2	6.6 E0	9.3 E-4
		Cl	0.91	0.029	4.4 E-1	--	74	7.7 E1	7.4 E0	2.0 E-3
	3	EC	--							
	15	EC	0.73	0.049	1.3 E0	--	98	9.9 E1	8.6 E-1	2.2 E-3
		Cl	0.78	0.045	9.9 E-1	--	98	9.9 E1	1.4 E0	2.0 E-3
	16	EC	--							
	17	EC	0.95	-0.051	2.7 E-5	--	14	5.2 E4	1.9 E9	5.1 E-6
		Cl	0.94	0.066	4.6 E-5	--	116	3.1 E4	6.8 E8	8.5 E-6
	19	EC	0.52	0.022	2.8 E-6	--	7	5.2 E5	1.9 E11	6.1 E-7
Mean			**0.83**	**0.015**			**70**	**7.5 E4**	**2.4 E10**	**1.1 E-3**
Gamma	1	EC	--							
		Cl	0.96	0.001	2.5 E-5	4.2 E-1	71	2.4 E4	9.6 E8	8.3 E-6
	2	EC	0.99	0.029	2.0 E-8	4.5 E-3	160	3.3 E5	1.6 E13	4.6 E-7
		Cl	0.90	0.013	8.9 E-6	4.8 E-3	75	8.5 E2	8.7 E7	1.8 E-4
	3	EC	--							
	15	EC	0.90	-0.006	6.6 E-7	4.7 E-1	32	7.2 E5	1.6 E12	2.1 E-7
		Cl	0.54	-0.148	1.9 E-6	4.2 E-1	145	2.3 E5	3.1 E-2	6.2 E-7
	16	EC	--							
	17	EC	0.97	-0.010	1.6 E-4	1.1 E0	38	9.8 E3	6.1 E7	2.7 E-5
		Cl	0.99	0.025	6.4 E-5	8.8 E-1	101	2.0 E4	3.0 E8	1.4 E-5
	19	EC	0.53	0.022	3.9 E-5	1.2 E0	4	4.5 E4	1.2 E9	7.0 E-6
Mean			**0.83**	**0.032**			**87**	**2.4 E5**	**2.3 E12**	**3.2 E-4**

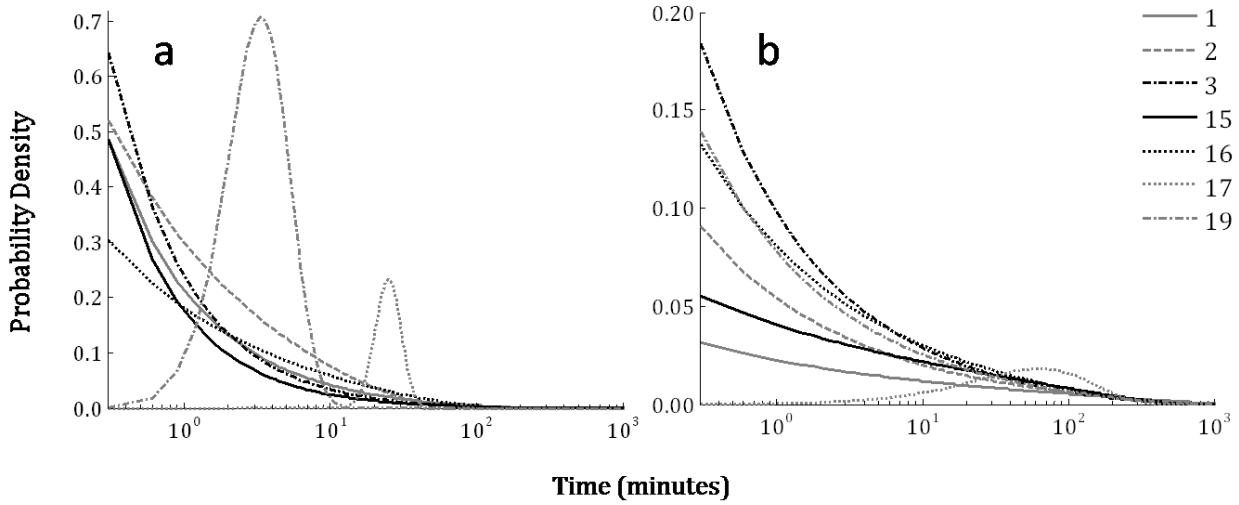

Figure 27: Gamma RTDs of pressure wave transport for each well based on best parameter estimates for experiments 1 (a) and 2 (b).

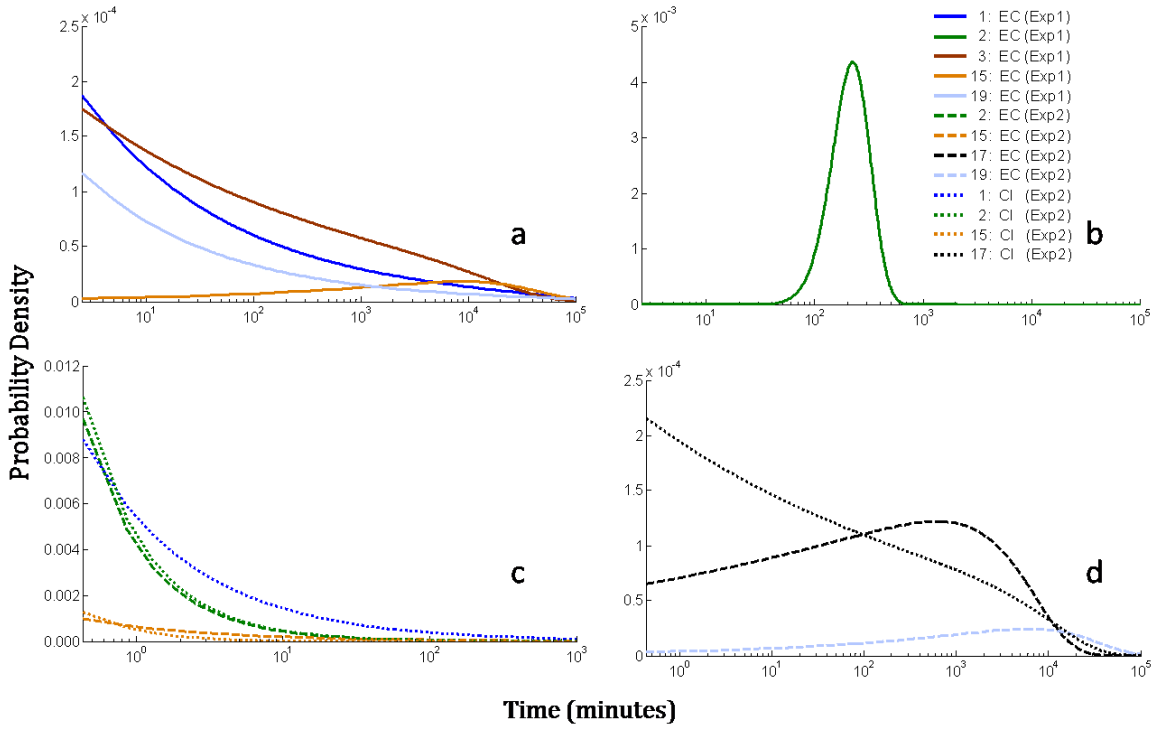

Figure 28: Gamma RTDs of tracer transport for each well based on best parameter estimates for experiments 1 (a & b) and 2 (c & d). Distributions are grouped by scale similarity.

DISCUSSION

Transport in field soils is affected by multiple factors, and in combination with spatial and temporal variability of subsurface hydrochemistry, the variation of chemical responses to forcing events is more than can be quantified from these experiments. Spatial variability in chemical response may be partially attributed to antecedent moisture conditions (Flury, 1994) and micro-topography (Weiler and Naef, 2003) which affect infiltration patterns and flowpaths. Temporal variability in chemical response among events reflect the dynamic nature of infiltration and transport mechanisms which are affected by water table characteristics, overstory and understory vegetation, ground cover, and burrowing organisms in the subsurface. Vegetation at the field site changed throughout the period of monitoring in response to periodic flooding, seasonal deciduousness, and trees uprooted and broken by tropical cyclones.

For simplification, we categorized subsurface water-chemistry responses to forcing events into three categories: new water response, old water response, or no response. Theories of storm runoff generation (Church, 1997; Jones et al., 2006) imply that new water responses are caused by bypass flow of event water and old water responses are caused by displacement of pre-event water by piston action, with new water effectively pushing old water into the well. A lack of chemical response in a well with a clear hydraulic response implies that water of the same chemical makeup entered the well in response to the forcing event. Each of these mechanisms apparently controlled chemical response to some degree in every event. Even within events, the direction of chemical responses sometimes changed from old water to new water. This behavior violated the three-category conceptual model and limited or precluded modeling. Sporadic input from intermittent pumping or rainfall and corresponding changes in subsurface hydraulic gradients may have contributed to this shifting behavior.

Although EC response was poorly correlated to hydraulic response in this study (Figure 20), water table irregularities and spatially variable hydraulic responses to forcing events are probably drivers of spatially-variable chemical response to some degree. For example, Jung et al (2004) found

that topographic depressions in floodplains are associated with groundwater domes that form as pooled water slowly infiltrates and creates a radial hydraulic gradient. At the scale of this study, a similar effect may have occurred in response to variable pooling and infiltration patterns. Additional factors that may contribute to an uneven water table include spatial variability of texture and structure and layered sediments such as relatively impermeable clay lenses (Figure 4). Nevertheless, because flow velocity is directly proportional to hydraulic gradient, even a large, 1-meter difference in hydraulic head between two wells would only account for one order of magnitude of travel time variability, assuming uniform hydraulic conductivity. Thus, although hydraulic micro-gradients likely had some effect on tracer transport rates, this mechanism cannot account for the five orders of magnitude variability of transport rates we measured.

The end member mixing analysis (EMMA) exposed limitations in our simple conceptual model of soil chemistry which defined old water as the maximum solute concentration measured in the soil during the period of record. The EMMA results indicated that the end members were not well-defined, because the observed well chemistry was outside the range of possibilities defined by simple mixing (Figure 10). The short period of chloride monitoring (about two weeks) indicated that "old" soil water chloride concentration was about 300 mg/L (Figure 21), but a more extensive investigation of soil water chemistry would almost certainly refine the definition of end members. An alternate assumption of chloride concentration of the soil water end member matching the chloride concentration of the bayou water end member would have constrained the majority of measurements within the prescribed chemical boundaries, particularly for the most apparently accurate sensors in wells 2 and 15.

Overall, behaviors of EC and chloride tracers are difficult to reconcile. During the active tracer test (experiment 2), EC and chloride data varied independently despite the fact that the two tracers are chemically related: the high EC in the reservoir was a direct result of the added KCl. However, even in the reservoir, the correlation between EC and chloride was imperfect (Figure 22). Chloride increased in response to pumping in all four wells where we measured it, but EC varied: increasing in two wells

(15 and 17) and decreasing or fluctuating in the remaining wells (2 and 1, respectively). With the limited data set, we can only postulate possible instrument problems or hydrochemical processes that might have produced these results. One possibility is that, because the EC sensors are less sensitive than are the chloride probes to instantaneous changes in the absence of constant flushing of the electrode, recorded changes in soil water EC lagged behind changes in chloride. Lack of correlation between EC and chloride data may have occurred if there was vertical stratification of water during experiment 2, either from chemical variability of laterally infiltrating soil water or from denser, KCl-laden water at the bottom of some wells; EC sensors were situated approximately 35 cm above chloride sensors in the wells.

Despite numerous unknowns, the transfer function model structure allowed quantification of the soil properties at the field scale. The benefit of using a linear system approach is that it does not require deterministic assumptions of transport mechanisms, which in the field is usually unknown or unknowable (Jury, 1982). A linear system model lumps complex processes into a probabilistic function of time or flow, so even though chemical and hydraulic residence time is largely dependent on the nature of flowpaths, we needed not measure them directly to infer their effective influence on solute transport (Sardin et al, 1991). The conclusions are based on these assumptions.

Confidence in modeled residence time distributions is limited by the accuracy and resolution of the defined input and response functions. One potentially important source of error is in the accuracy of the baselines defined for tracer and pressure wave response functions. The model fits of the tails of the pressure wave breakthrough curves (late-time data) were most sensitive to this interpretation. For tracer modeling, head differential time stopped when the reservoir drained, so we did not capture the tails of the breakthrough curves, and the shape of tracer response curves is less sensitive to interpretation.

Differences in pressure wave and tracer transport residence time distributions highlight the importance of using tracers when characterizing subsurface connectivity, because the hydraulic models alone described less of the total variability. Pressure wave RTDs describe the transport of

energy through the natural levee, and tracer RTDs describe the transport of mass (Vache and McDonnell, 2006). The greater spatial variability of tracer RTDs in comparison to pressure wave RTDs indicates multple functioning mechanisms of hydraulic response within the natural levee. Shorter mean residence times and faster transport velocities in some wells suggest preferential flow occurred during our experiments. Additionally, spatial disparity in the magnitude of chemical response (Figure 26) suggests that some wells were more directly connected to event water in the subsurface.

We observed more variability at the scale of the well field than at any individual well; therefore, in characterizing flow mechanisms in natural levee sediments, the scale at which transport is observed is paramount. At the outset of this study, slug tests (Bouwer, 1989; Bouwer and Rice, 1976) at two separate points in the vicinity of our study site measured a mean hydraulic conductivity (K) of 1.9 E-7 m/s. Estimated mean velocities from the RTDs and measured head gradients in the tracer tests gives a minimum K (7.3 E-5 m/s) two orders of magnitude larger and a grand mean K (0.14 m/s) seven orders of magnitude larger than the slug test K. This result supports the prevailing paradigm (Beven and Germann, 1982) that Darcy's law approaches are insufficient to describe water flow at field scales, because they treat the soil as a homogenous matrix and neglect the influence of preferential flow. At a large field scale (approximately 10,000 m^2) in a forested riparian wetland, Elci and Moltz (2008) found mean K measured by a tracer experiment two orders of magnitude larger than measured by slug tests.

Residence time distributions of chemical tracers at the large scale and small imposed gradients we measured provide representative estimates of spatially variable flow rates and mechanisms in natural levee sediments, because hydraulic gradients in riverine wetlands tend to be ephemeral and small. Results suggest that in a common geomorphic and hydraulic setting, subsurface connections between backswamps and bayous may have significant biological and biogeochemical implications. The problem of the appropriate scale for measuring and applying hydraulic properties is an area of unresolved research. Often processes governing subsurface water flow at small scales are overwhelmed by larger scale patterns, and processes that drive large-scale patterns are diffused by

small-scale mechanisms (Zeleke and Si, 2005). Situated somewhere between a basin scale and a soil core scale, our experiment can be considered a mesoscale study. Because extrapolating hydraulic properties to scales outside those in which they were directly measured is problematic, these measurements may be particularly useful, as they are directly applicable to a scale that is often the focus of management applications.

CONCLUSIONS

Higher spatial variability of chemical residence times in comparison to pressure wave residence times indicates differential functioning mechanisms of mass verses energy transport, and higher variability of functioning mass transport mechanisms suggests that preferential flowpaths affect water and solute transport. At the scale of these experiments, hydraulic conductivities (*K*) were greater than estimated by standard slug tests in all cases. High *K* and large spatial and temporal variability in transport rates are likely the result of preferential flowpaths that allow water and tracer to bypass a large portion of the soil volume. Because the important influence of preferential flowpaths on water and solute transport in riverine wetlands is not captured by small-scale measurements, methods that estimate transport rates based on small-scale measurements likely greatly underestimate transport rates at the mesoscale. Specifically, we conclude the following concerning mesoscale transport in rapidly aggrading riverine wetland natural levees:

- Mean subsurface flow velocities of pressure waves (energy) are faster than tracer (mass) velocities. In our study, transport velocities between the two differed by two orders of magnitude (2.5 E-2 and 3.2 E-4 m/s, respectively).
- Spatial variability of tracer transport velocities is large: between 1.6 E-7 and 6.8 E-5 m/s (0.01 and 5.9 m/day) under a mean hydraulic gradient of 12 cm and between 2.1 E-7 and 2.2 E-3 m/s (0.02 and 190 m/day) under a mean hydraulic gradient of 70 cm.
- High spatial and temporal variability of chemical response and tracer residence time distributions compared hydraulic response and pressure wave residence time distributions suggest that preferential flow paths affect mass transport but do not consistently reoccur in space or time.

REFERENCES

Aslan, A. and Autin, W.J., 1998. Holocene flood-plain soil formation in the southern lower Mississippi Valley: Implications for interpreting alluvial paleosols. Geological Society of America Bulletin, 110: 433-449.

Barron, A., 1996. Thesis. Acidification of Poorly Drained Backswamp Soils in the Mississippi River Floodplain Due To Reduced Sulphur Oxidation, Louisiana State University, 103 pp.

Beven, K. and Germann, P., 1982. Macropores and Water-flow in Soils. Water Resources Research, 18: 1311-1325.

Bouma, J., 1991. Influence of Soil Macroporosity on Environmental Quality. Advances in Agronomy, 46: 1-37.

Bouwer, H., 1989. The Bouwer and Rice Slug Test – An Update. Ground Water, 27: 304-309.

Bouwer, H. and Rice, R.C., 1976. Slug Test for Determing Hydraulic Conductivity of Unconfined Aquifers with Completely or Partially Penetrating Wells. Water Resources Research, 12: 423-428.

Buttle, J.M., 1994. Isotope Hydrograph Separations and Rapid Delivery of Pre-event Water from Drainage Basins. Progress in Physical Geography, 18(1): 16-41.

Cazanacli, D. and Smith, N.D., 1998. A study of morphology and texture of natural levees - Cumberland Marshes, Saskatchewan, Canada. Geomorphology, 25: 43-55.

Church, M.R., 1997. Hydrochemistry of forested catchments. Annual Review of Earth and Planetary Sciences, 25: 23-59.

Deegan, L.A., Kennedy, H.M. and Neill, C., 1984. Natural Factors and Human Modifications Contributing to Marsh Loss in Louisiana Mississippi River Deltaic Plain. Environmental Management, 8: 519-527.

Demas, C.R., S. R. Brazelton & N. J. Powell, 2002. The Atchafalaya Basin - river of trees, U.S. Geological Survey.

Dooge, J., 1973. Linear theory of hydrologic systems. Agricultural Research Service, US Dept. of Agriculture, 327 pp.

Duffy, C.J. and Gelhar, L.W., 1985. A Frequency-domain Approach to Water-quality Modeling in Groundwater- Theory. Water Resources Research, 21: 1175-1184.

Elci, A. and Molz, F.J., 2008. Identification of Lateral Macropore Flow in a Forested Riparian Wetland through Numerical Simulation of a Subsurface Tracer Experiment. Water Air and Soil Pollution, 197: 149-164.

Filgueira-Rivera, M., Smith, N.D. and Slingerland, R.L., 2007. Controls on natural levee development in the Columbia river, British columbia, Canada. Sedimentology, 54: 905-919.

Fisk, H.N., 1947. Fine-grained alluvial deposits and their effect on Mississippi River activity U.S. Army Corps of Engineers, Mississippi River Commission, Vicksburg, Mississippi.

Fisk, H.N., 1952. Geological Investigation of the Atchafalaya Basin and the Problem of Mississippi River Diversion, U.S. Army Corps Engineers, Mississippi River Committee, Vicksburg, Mississippi.

Fisk, H.N., 1944. Geological Investigation of the Alluvial Valley of the Lower Mississippi River. Mississippi River Committee, Vicksburg, Mississippi.

Fitzgerald, D.F., Price, J.S. and Gibson, J.J., 2003. Hillslope-swamp interactions and flow pathways in a hypermaritime rainforest, British Columbia. Hydrological Processes, 17: 3005-3022.

Flury, M., Fluhler, H., Jury, W.A. and Leuenberger, J., 1994. Susceptibility of Soils to Preferential Flow of Water - A Field-Study. Water Resources Research, 30: 1945-1954.

Frazier, D.E., 1967. Recent deltaic deposits of the Mississippi River, their development and chronology. Trans. Gulf Coast Assoc. Geol. Soc., 17 287–315.

Gerke, H.H. and Van Genuchten, M.T., 1993. A Dual-Porosity Model for Simulating the Preferential Movement of Water and Solutes in Structured Porous-media. Water Resources Research, 29: 305-319.

Gish, T.J. and Jury, W.A., 1983. Effect of Plant-roots and Root Channels on Solute Transport. Transactions of the ASAE, 26: 440-444.

Grimm, N.B. and Fisher, S.G., 1984. Exchange Between Interstitial and Surface-water Implications for Stream Metabolism and Nutrient Cycling. Hydrobiologia, 111: 219-228.

Hall, F.R. and Moench, A.F., 1972. Application of Convolution Equation to Stream-Aquiver Relationships. Water Resources Research, 8: 487-493.

Harvey, J.W. and Nuttle, W.K., 1995. Fluxes of Water and Solute in a Coastal Wetland Sediment .2. ffect of Macropores on Solute Exchange with Surface-water. Journal of Hydrology, 164: 109-125.

Hewlett, J.D., 1982. Principles of Forest Hydrology. The University of Georgia Press, Athens, 183 pp.

Hillel, D. and Baker, R.S., 1988. A Descriptive-Theory of Fingering During Infiltration into Layered Soils. Soil Science, 146: 51-56.

Hooper, R.P., Christophersen, N. and Peters, N.E., 1990. Modeling Streamwater Chemistry as a Mixture of Soilwater End-members - An Application to the Panola Mountain Catchment, Georgia, USA. Elsevier Science Bv, pp. 321-343.

Hopkinson, C.S. and Day, J.W., 1980. Modeling Hydrology and Eutrophication in a Louisiana Swamp Forest Ecosystem. Environmental Management, 4: 325-335.

Horton, R.E., 1933. The role of infiltration in the hydrologic cycle. Transactions-American Geophysical Union, 14: 446-460.

Hupp, C.R., 2000. Hydrology, geomorphology and vegetation of Coastal Plain rivers in the south-eastern USA. Hydrological Processes, 14: 2991-3010.

Hupp, C.R., Demas, C.R., Kroes, D.E., Day, R.H. and Doyle, T.W., 2008. Recent sedimentation patterns within the central Atchafalaya Basin, Louisiana. Wetlands, 28: 125-140.

Johnston, C.A., Bridgham, S.D. and Schubauer-Berigan, J.P., 2001. Nutrient dynamics in relation to geomorphology of riverine wetlands. Soil Science Society of America Journal, 65: 557-577.

Jones, J.P., Sudicky, E.A., Brookfield, A.E. and Park, Y.J., 2006. An assessment of the tracer-based approach to quantifying groundwater contributions to streamflow. Water Resources Research, 42: 15.

Jung, M., Burt, T.P. and Bates, P.D., 2004. Toward a conceptual model of floodplain water table response. Water Resources Research, 40: 13.

Junk WJ, Bayley PB, Sparks RE. 1989. Theflood pulse concept in river-floodplain systems.Canadian Special Publication of Fisheries and Aquatic Sciences 106: 110-127.

Jury, W.A., 1982. Simulation of Solute Transport Using a Transfer-function Model. Water Resources Research, 18: 363-368.

Kabat, P., Hutjes, R.W.A. and Feddes, R.A., 1997. The scaling characteristics of soil parameters: From plot scale heterogeneity to subgrid parameterization. Journal of Hydrology, 190: 363-396.

Keim, R.F. and Skaugset, A.E., 2004. A linear system model of dynamic throughfall rates beneath forest canopies. Water Resources Research, 40: 12.

Kirchner, J.W., Feng, X.H. and Neal, C., 2001. Catchment-scale advection and dispersion as a mechanism for fractal scaling in stream tracer concentrations. Journal of Hydrology, 254: 82-101.

Kresic, N., 2007. Hydrogeology and Groundwater Modeling. . CRC Press, Boca Raton, FL, 807 pp.

Lagarias, J.C., Reeds, J.A., Wright, M.H. and Wright, P.E., 1998. Convergence properties of the Nelder-Mead simplex method in low dimensions. Siam Journal on Optimization, 9: 112-147.

Legates, D.R. and McCabe, G.J., 1999. Evaluating the use of "goodness-of-fit" measures in hydrologic and hydroclimatic model validation. Water Resources Research, 35: 233-241.

Legout, A., Legout, C., Nys, C. and Dambrine, E., 2009. Preferential flow and slow convective chloride transport through the soil of a forested landscape (Fougeres, France). Geoderma, 151: 179-190.

Lin, K.R., Guo, S.L., Zhang, W.H. and Liu, P., 2007. A new baseflow separation method based on analytical solutions of the Horton infiltration capacity curve. Hydrological Processes, 21: 1719-1736.

Liu, G.S., Zheng, C.M. and Gorelick, S.M., 2007. Evaluation of the applicability of the dual-domain mass transfer model in porous media containing connected high-conductivity channels. Water Resources Research, 43(12).

Luxmoore, R.J. and Ferrand, L.A., 1993. Towards a Pore-Scale Analysis of Preferential Flow and Chemical Transport. In: D. Russo and G. Dagan (Editors), Water Flow and Solute Transport in Soils: Developments and Applications, Heidelberg, Germany.

Malard, F., Tockner, K., Dole-Olivier, M.J. and Ward, J.V., 2002. A landscape perspective of surface-subsurface hydrological exchanges in river corridors. Freshwater Biology, 47: 621-640.

Maloszewski, P. and Zuber, A., 1998. A general lumped parameter model for the interpretation of tracer data and transit time calculation in hydrologic systems - Comments. Journal of Hydrology, 204: 297-300.

McGuire, K.J., DeWalle, D.R. and Gburek, W.J., 2002. Evaluation of mean residence time in subsurface waters using oxygen-18 fluctuations during drought conditions in the mid-Appalachians. Journal of Hydrology, 261: 132-149.

Meinzer, O.E., 1932 (reprint 1959). Outline of methods for estimating ground-water supplies. Contributions to the hydrology of the United States, U.S. Geological Survey, Washington, D.C.

Murphy, K.E., Touchet, B.A., White, A.G., Daigle, J.J. and Clark, H.L., 1977. Soil survey of St. Martin Parish, Louisiana, US Department of Agriculture, Soil Conservation Service, in cooperation with the Louisiana Agricultural Experiment Station, Washington, DC.

Nash, J.E. and Sutcliffe, J.V., 1970. River Flow Forecasting through conceptual models, I, A discussion of principles. Journal of Hydrology, 10: 282-290.

Noguchi, S., Tsuboyama, Y., Sidle, R.C. and Hosoda, I., 1999. Morphological characteristics of macropores and the distribution of preferential flow pathways in a forested slope segment. Soil Science Society of America Journal, 63: 1413-1423.

Nobles, M.M., Wilding, L.P. and McInnes, K.J., 2004. Pathways of dye tracer movement through structured soils on a macroscopic scale. Soil Science, 169: 229-242.

Parsons, D.F., Hayashi, M. and van der Kamp, G., 2004. Infiltration and solute transport under a seasonal wetland: bromide tracer experiments in Saskatoon, Canada. Hydrological Processes, 18: 2011-2027.

Poole, G.C., Stanford, J.A., Frissell, C.A. and Running, S.W., 2002. Three-dimensional mapping of geomorphic controls on flood-plain hydrology and connectivity from aerial photos. Geomorphology, 48: 329-347.

Roberts, H.H., 1998. Delta switching: Early responses to the Atchafalaya River diversion. Journal of Coastal Research, 14: 882-899.

Sabo, M.J., Bryan, C.F., Kelso, W.E. and Rutherford, A., 1999. Hydrology and aquatic habitat characteristics of a riverine swamp: I. Influence of flow on water temperature and chemistry. Regulated Rivers-Research & Management, 15: 505-523.

Sardin, M., Schweich, D., Leij, F.J. and Vangenuchten, M.T., 1991. Modeling the Nonequilibrium Transport of Linearly Interacting Solutes in Porous-media. Water Resources Research, 27: 2287-2307.

Seyfried, M.S. and Wilcox, B.P., 1995. Scale and the Nature of Spatial Variability – Field Examples Having Implications for Hydrologic Modeling. Water Resources Research, 31: 173-184.

Sidle, R.C., Noguchi, S., Tsuboyama, Y. and Laursen, K., 2001. A conceptual model of preferential flow systems in forested hillslopes: evidence of self-organization. Hydrological Processes, 15: 1675-1692.

Sklash, M.G., Beven, K.J., Gilman, K. and Darling, W.G., 1996. Isotope studies of pipeflow at Plynlimon, Wales, UK. Hydrological Processes, 10: 921-944.

Smith, L.M., J. B. Dunbar, and L. D. Britsch, 1985. Geomorphological investigation of the Atchafalaya Basin, Area West, Atchafalaya Delta, and Terrebonne Marsh, U.S. Army Corps Engineers, Waterway Experimental Station.

Triska, F.J., Duff, J.H. and Avanzino, R.J., 1993. The Role of Water Exchange Between a Stream Channel and its Hyporheic Zone and Nitrogen Cycling at the Terrestrial Aquatic Interface. Hydrobiologia, 251: 167-184.

Tye, R.S. and Coleman, J.M., 1989. Depositional Processes and Stratigraphy of Fluvially Dominated Lacustrine Deltas - Mississippi Delta Plain. Journal of Sedimentary Petrology, 59: 973-996.

Vache, K.B. and McDonnell, J.J., 2006. A process-based rejectionist framework for evaluating catchment runoff model structure. Water Resources Research, 42(2).

Vereecken, H., Kasteel, R., Vanderborght, J. and Harter, T., 2007. Upscaling hydraulic properties and soil water flow processes in heterogeneous soils: A review. Vadose Zone Journal, 6: 1-28.

Wang, H., 2002. Thesis. Describing and Predicting Breakthrough Curves for non-Reactive Solute Transport in Statistically Homogeneous Porous Media. Virginia Polytechnic Institute and State University, 190 pp.

Weiler, M. and Naef, F., 2003. Simulating surface and subsurface initiation of macropore flow. Journal of Hydrology, 273: 139-154.

Wilson, G.V. and Luxmoore, R.J., 1988. Infiltration, Macroporosity, and Mesoporosity Distributions on Two Foreted Watersheds. Soil Science Society of America Journal, 52: 329-335.

Xin, P., Jin, G.Q., Li, L. and Barry, D.A., 2009. Effects of crab burrows on pore water flows in salt marshes. Advances in Water Resources, 32: 439-449.

Zeleke, T.B. and Si, B.C., 2005. Scaling relationships between saturated hydraulic conductivity and soil physical properties. Soil Science Society of America Journal, 69: 1691-1702.

APPENDIX A: WATER LEVEL BASELINES

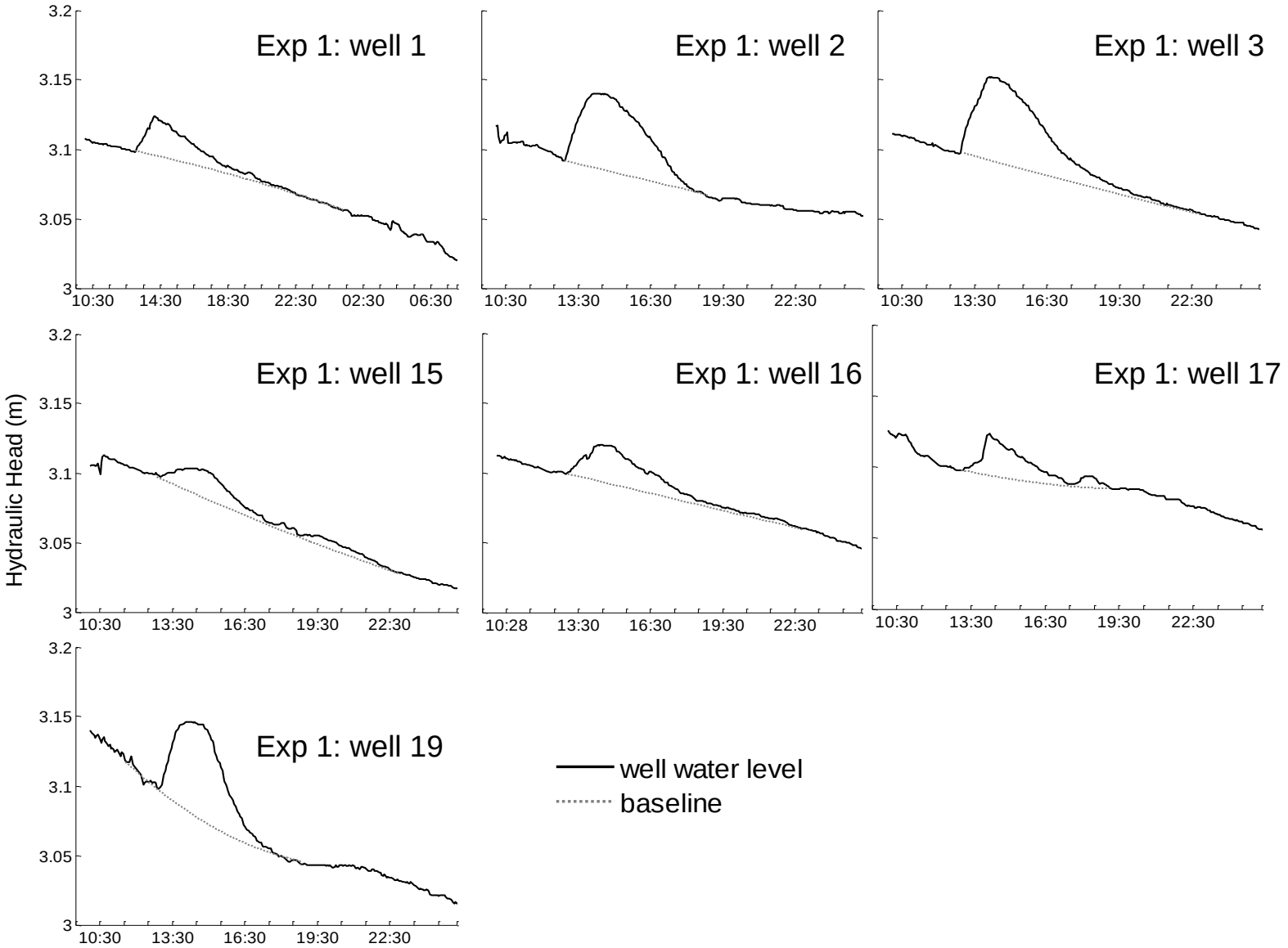

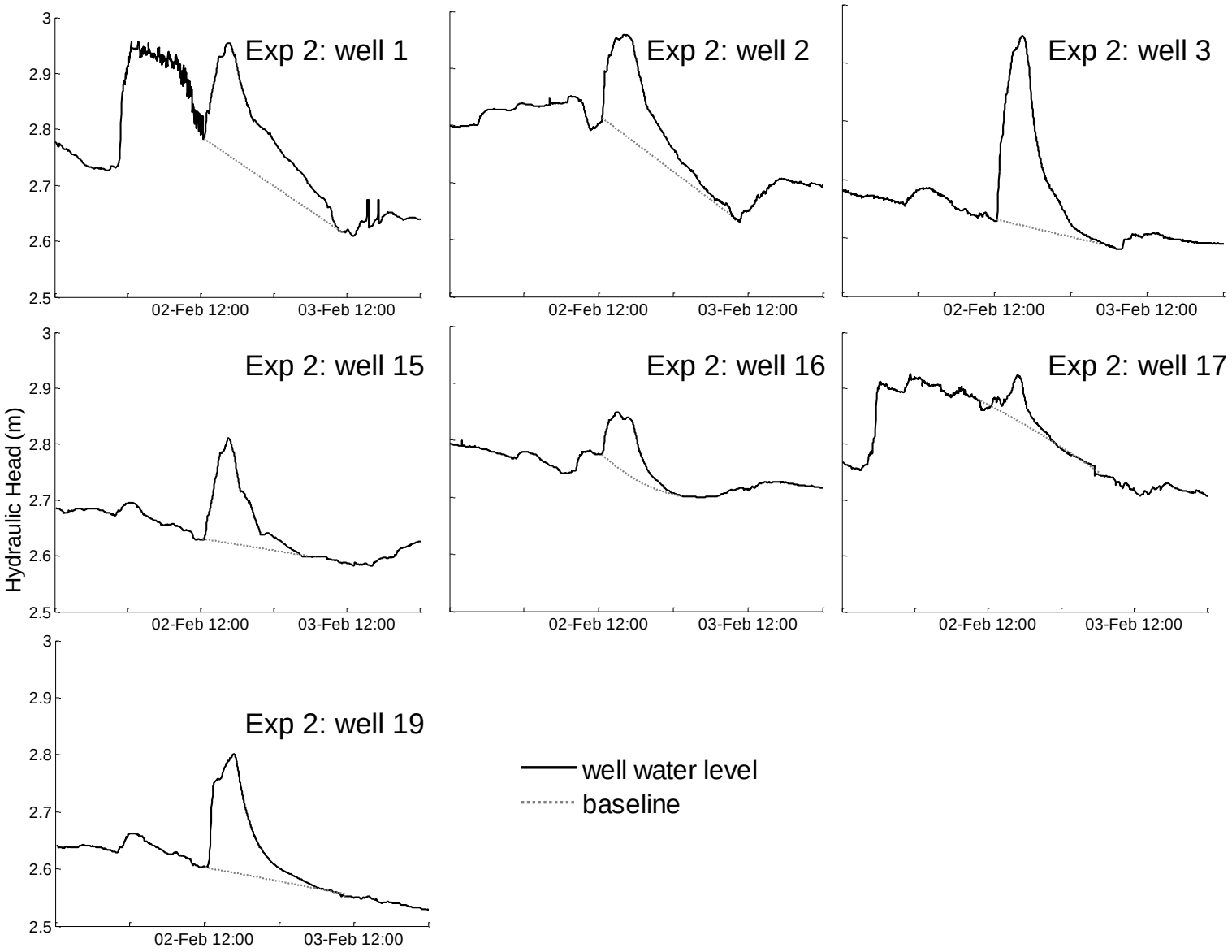
Exp 2: well 1
Exp 2: well 2
Exp 2: well 3
Exp 2: well 15
Exp 2: well 16
Exp 2: well 17
Exp 2: well 19
Hydraulic Head (m)
3
2.9
2.8
2.7
2.6
2.5
02-Feb 12:00
03-Feb 12:00
well water level
baseline

APPENDIX B: OPTIMIZED MODELS OF PRESSURE WAVE TRANSPORT BASED ON BEST-FIT PARAMETERS.

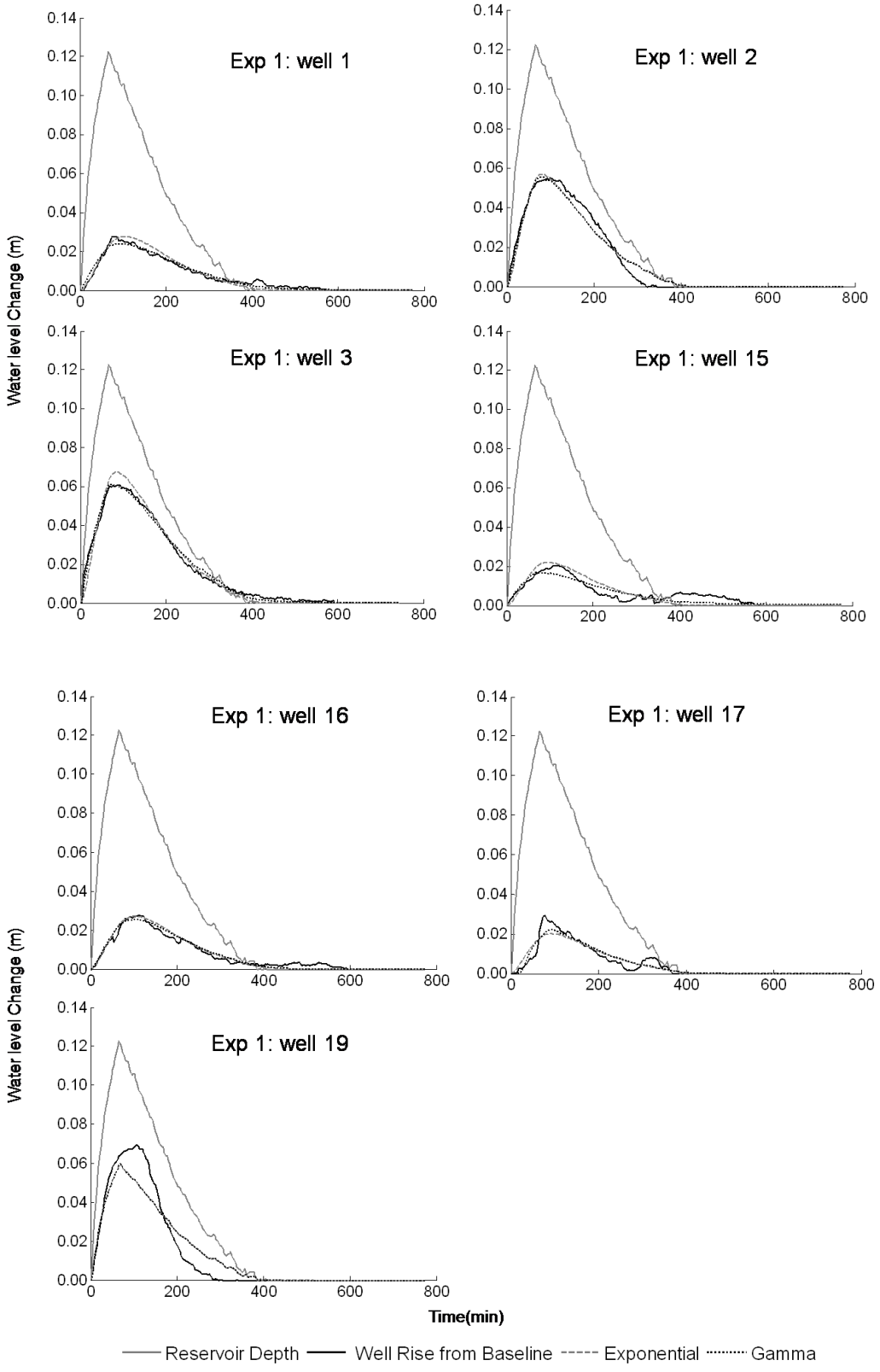

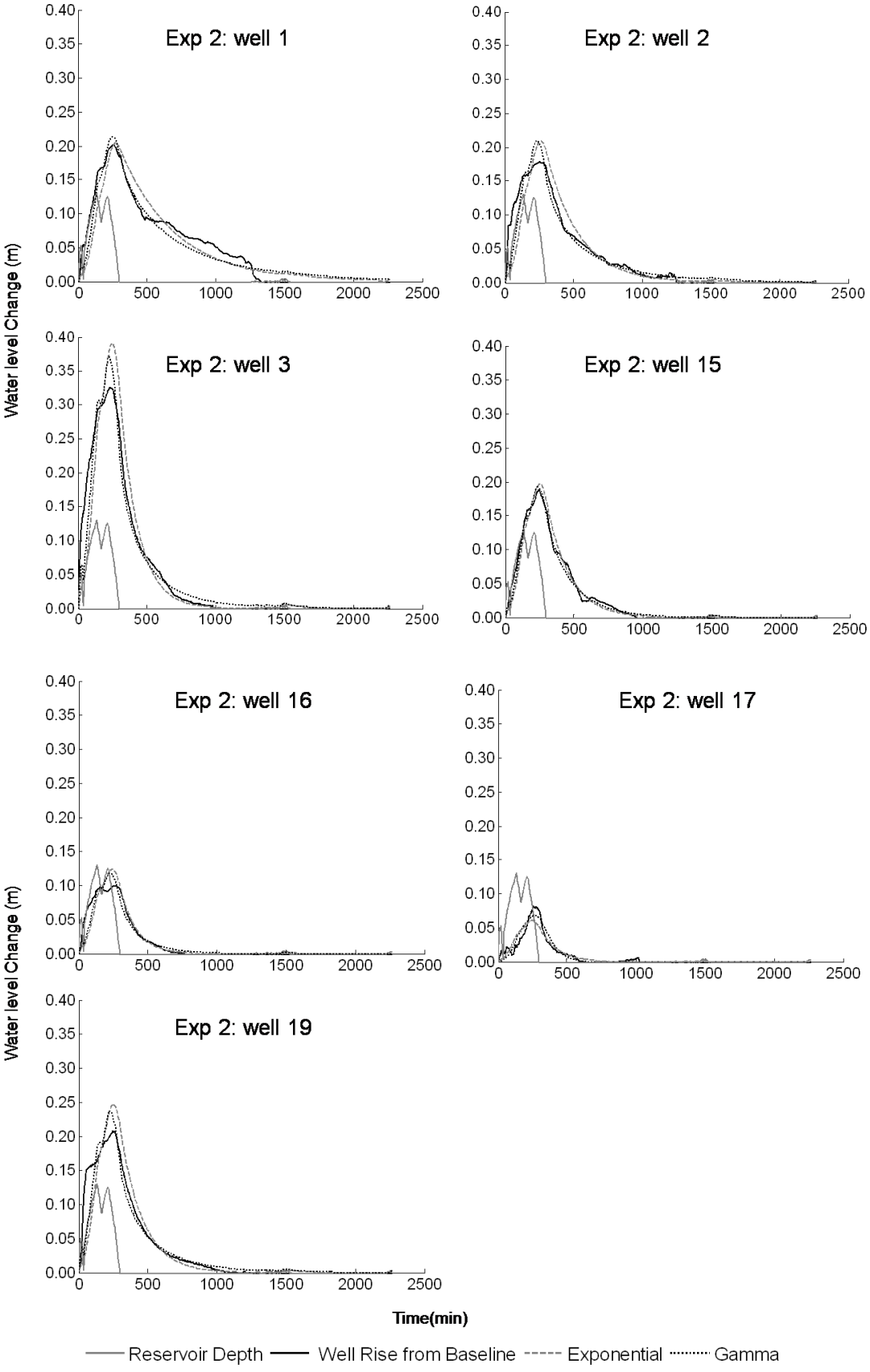
Exp 2: well 1
Exp 2: well 2
Exp 2: well 3
Exp 2: well 15
Exp 2: well 16
Exp 2: well 17
Exp 2: well 19
Water level Change (m)
Time(min)
Reservoir Depth
Well Rise from Baseline
Exponential
Gamma

VITA

April Newman earned a Batchelors of Science. in environmental studies from the University of Nevada Las Vegas in 2002 where she first gained an interest and respect for wetlands while working as an undergraduate research assistant at a constructed desert wetland. After a summer internship with a restoration ecologist at the Las Vegas Springs Preserve, Ms. Newman moved to southwest Oregon where she worked for three years as a field technician and forest hydrologist at the US Bureau of Land Management. Evaluating headwater streams in mountainous watersheds stimulated her curiosity about surface-groundwater interactions and connectivity, so she eventually left her job for a graduate research assistantship in the School of Renewable Natural Resources at Louisiana State University that provided an opportunity to combine her interests in wetlands, hydrology, and forests. After graduating with a Master of Science degree, Ms. Newman intends to continue research on the processes and implications of hydrologic connectivity in wetlands and forests and hopes to someday apply her knowledge and skills to solve real-world environmental problems.